BUSITEMA UNIVERSITY

FACULTY OF ENGINEERING AND TECHNOLOGY

DEPARTMENT OF POLYMER, TEXTILE AND INDUSTRIAL ENGINEERING

FINAL YEAR PROJECT

SYNTHESIS OF CHITOSAN MODIFIED ROTTEN BAGASSE BIOCHAR FOR LEAD (II) IONS REMOVAL FROM INDUSTRIAL PAINT WASTEWATER

By

MUTYABA FAHADI (BU/UG/2022/1568)

&

LATABO JACQULINE (BU/UG/2022/1397)

MAY, 2026

FINAL YEAR PROJECT REPORT

SYNTHESIS OF CHITOSAN MODIFIED ROTTEN BAGASSE BIOCHAR FOR LEAD (II) IONS REMOVAL FROM INDUSTRIAL PAINT WASTEWATER

By

MUTYABA FAHADI

(BU/UG/2022/1568)

&

LATABO JACQULINE

(BU/UG/2022/1397)

SUPERVISORS

PROF. NIBIKORA ILDEPHONSE

MR. TIGALANA DAN

MR. ANKWATSA JORAM

This final year project report is submitted to the Faculty of Engineering and technology in partial fulfilment of the requirement for the award of the degree of Bachelor of Science in Polymer Textile and Industrial Engineering of Busitema University

ABSTRACT

Lead (II) ions presence in industrial wastewater poses a critical environmental and public health challenge where paint manufacturing industries discharge effluents containing lead concentration as high as 3.88mg/L far exceeding the NEMA permissible limit of 01mg/L and the WHO drinking water guideline of 0.01mg/L. conversional remediation techniques such as chemical precipitation, ion exchange, reverse osmosis and electrochemical reduction are effective but very costly, energy intensive and produce possible secondary pollutants creating an urgent need for low-cost, locally viable and environmentally sustainable alternatives. This study therefore synthesised and evaluated a chitosan modified rotten bagasse biochar as an adsorbent for the selective and efficient removal of lead (II) ions from real industrial paint wastewater. Sugar cane was subjected to anaerobic biodegradation for 2 months to enhance porosity and mineral content, then pyrolysed under limited oxygen at 600℃ for 2 hours to produce RBB which was subsequently modified with chitosan. The bio composite adsorbent was characterised using SEM-EDX and FTIR which revealed the presence of mineral elements due to decomposition and increased surface function groups (-NH2 and -OH) after chitosan modification suggesting ion exchange and surface complexation during adsorption. Optimal adsorption conditions were established at an adsorbent dosage of 1.65g, pH of 6.7 and contact time of 80 minutes with predicted maximum removal efficiency of 87.4% and an equilibrium adsorption capacity of 1.835mg/g which was superior to both pristine RBB (1.23mg/g) and Ch-RBB (1.49 mg/g). Adsorption kinetics were best described by the PSO model with R2 = 0.988 which confirmed chemisorption as the dominant rate controlling mechanism while Boyd model analysis indicated that film diffusion governs the initial adsorption stage and intraparticle diffusion controls the later stage, together constituting a multi stage diffusion controlled process.

DECLARATION

I MUTYABA FAHADI with LATABO JACQULINE declare that this research report has been compiled by us and has never been used for any academic reward at any institute of learning or level of education.

Signature; ……………………….

Date; 29/05/2026

Signature; ……………………….

Date; 29/05/2026

APPROVAL

This report has been written under the supervision of the following supervisors

PROF. NIBIKORA ILDEPHONSE

Signature; ______________________

Date; 02/06/2026

MR. TIGALANA DAN

Signature ·

Date: **2nd June, 2026**

MR. ANKWATSA JORAM

Signature

Date; **02/06/2026**

DEDICATION

We dedicate this project to all those involved in sustainable manufacturing and environment remediation through sustainable waste management.

ACKNOWLEDGEMENT

We are so much grateful and thankful for God's providence and guidance through our research and compilation of this research. We highly appreciate our parents and guardians for their unwavering financial, spiritual and moral support in making our academic journeys walkable. We also extend our sincere gratitude to our supervisors for the knowledge and guidance and to our fellow course mates who have also endlessly assisted in all times of need.

TABLE OF CONTENTS

ABSTRACT...i

DECLARATION ii

APPROVAL iii

DEDICATION..iv

ACKNOWLEDGEMENT v

TABLE OF CONTENTS...vi

LIST OF TABLES x

LIST OF FIGURES xi

List of acronyms xii

1 CHAPTER ONE: INTRODUCTION 1

1.1 Background 1

1.2 PROBLEM STATEMENT 3

1.3 Objectives of the study..4

1.3.1 Main objective 4

1.3.2 Specific objectives 4

1.3.3 Research questions..4

1.3.4 Justification of the study 5

1.3.5 Significance...6

1.3.6 Scope of the study 7

2 CHAPTER TWO: LITERATURE REVIEW 8

2.1 Sources and effect of Lead ions in the environment 8

2.2 Physiochemical properties of paint wastewater 8

2.3 Sugarcane bagasse as a biomass resource 9

2.4 Biochar properties 9

2.5 Effect of natural rotting as a pretreatment for biomass 10

2.6 Modification with chitosan 10

2.7 Methods of removing Lead ions from wastewater 11

2.7.1 Chemical precipitation 11

2.7.2 Ion exchange 11

2.7.3 Reverse osmosis 12

2.7.4 Coagulation 12

2.7.5 Electrochemical reduction 12

2.7.6 Adsorption 12

2.8 Adsorption mechanisms 13

2.9 Characterisation of modified rotten bagasse biochar 13

2.9.1 SEM-EDX 13

2.9.2 FTIR 14

2.10 Response surface methodology 15

2.11 Residual analysis 16

2.11.1 Predicted versus actual plot 16

2.11.2 Normal probability plot of residuals 16

2.11.3 Residual versus predicted values plot 17

2.11.4 Cook's distance plot...17

2.11.5 Residuals versus run order plot...17

2.11.6 Box-cox plot...18

2.12 Adsorption kinetics 18

3 CHAPTER THREE: METHODOLOGY 20

3.1 Preparation and modification of fresh and rotten bagasse biochar 20

3.2 Characterisation of FBB, RBB, CH-FBB and CH-RBB 20

3.3 Collection and characterisation of paint wastewater 21

3.4 Batch experiments...22

3.4.1 Adsorption process...22

3.4.2 Measuring concentration of lead (ii) ions at equilibrium................................23

3.5 Adsorption rate of Pb (II) on to CH-RBB..23

4 CHAPTER FOUR: RESULTS AND DISCUSSION 25

4.1 Biochar characterisation...25

4.1.1 Surface structure of rotten and modified and loaded biochar. 25

4.1.2 Surface functional groups of biochar 28

4.2 Paint wastewater Characterisation 29

4.3 Modelling and optimisation 30

4.3.1 Response surface methodology -BBD 30

4.3.2 Analysis of variables (ANOVA) 30

4.3.3 Residual analysis 32

4.3.4 Optimisation of adsorption conditions 33

4.3.5 Analysis of variable interactions 34

4.3.6 Effect of independent adsorption variables on removal of lead ions 35

4.4 Adsorption kinetic 37

5 CHAPTER 5 39

5.1 CONCLUSIONS 39

5.2 RECOMMENDATIONS 40

REFERENCES 41

APPENDICES 49

Appendix A: Biochar production process 49

Appendix B: Equipment used 50

Appendix C: Experiments 51

LIST OF TABLES

Table 3.1: Independent variables for Design of experiment..22

Table 3.2: Nonlinear equations for adsorption kinetic model..24

Table 4.1: Removal efficiency of Pb (II) ions under various conditions.................................30

Table 4.2: ANOVA for Reduced Quadratic model 31

Table 4.3: Adsorption kinetics constants...37

LIST OF FIGURES

Figure 4.1: SEM image for RBB (a), EDX graph for RBB (b) 25

Figure 4.2: SEM image for Chitosan rotten bagasse biochar (c), EDX image Ch-RBB (c), EDX image for Ch-RBB (d) 26

Figure 4.3: SEM image for Pb-Ch-RBB (e), EDX image for Pb-Ch-RBB (f) 27

Figure 4.4: FT/IR graph showing functional groups on RBB, Ch-RBB and Pb-Ch-RBB 29

Figure 4.5: Residual analysis for RSM-BBD model;(a) predicted vs actual removal efficiency, (b) cook’s distance plot, (c) Box-cox plot, (d) Residuals vs run number, (e) Residuals vs predicted removal efficiency, (f) Normal probability plot. 32

Figure 4.6: Predicted removal values after optimisation 34

Figure 4.7:Interaction effects of variables on Pb (II) ions removal; (a) AB, (b) AC, (c) BC..34

Figure 4.8: One factor effect; (a) R.E Vs A, (b) R.E Vs B, (c) R.E Vs C 35

Figure 4.9: Kinetic models, (a) Non linear pseudo first, second and intraparticle diffusion, (b) Boyd model...38

Figure A.0.1: Biochar production process 49

Figure B.0.2&2: HI9146 Dissolved Oxygen meter and JEN WAY 6705 Vis Spectrophotometer 50

Figure B.3&0.3: Ex Stick EC500 ph. Conductivity meter and Orbital Shaker SSL 50

FigureC.0.4&6: Extracting a yellow complex of $Pb(I)_2$ and Operating Vis's Spectrophotometer 51

FigureC.0.5: Filtration after adsorption experiments...51

List of acronyms

SDG- Sustainable development Goals

WHO- World Health Organisation

SEM EDX – Scanning Electron Microscopy and Energy Dispersive X-ray spectroscopy

FTIR – Fourier Transform Infrared spectroscopy

RBB – Rotten Bagasse Biochar

Ch-RBB – Chitosan Rotten Bagasse Biochar

Pb - Ch-RBB - Chitosan Rotten Bagasse Biochar loaded with Lead

NEMA- National Environment and Management Authority

RSM-BBD – Response surface methodology – Box Behnken Design

1 CHAPTER ONE: INTRODUCTION

1.1 Background

Lead contamination in industrial wastewater represents one of the most pressing environment and public health challenges confronting developing nations. In Uganda's paint manufacturing sector, inorganic pigments such as lead chromate and lead carbonate are widely used which results in their significant presence in process effluents. At the global scale, paint industries are among the most water-intensive manufacturing operations yet a substantial proportion of generated wastewater is discharged without adequate treatment (Nair K et al., 2021). The consequences of untreated lead bearing effluents entering waterbodies are severe even at trace concentrations, several researchers have reported that lead impair neurological development in children, elevate systolic blood pressure, induce anaemia and cause progressive kidney dysfunction n adults (Collin et al., 2022).

Conventional physicochemical methods like use of metal organic frameworks and chemical precipitation for removal of lead from wastewater have been used in industries. However these methods are having a lot of constraints like high operational costs, energy demands, secondary pollution associated with sludge disposal and reduces performance at low metal concentrations making them inaccessible to small and medium-scale industries (Goel, 2024). Because of this, major focus is given on the use of biological methods especially biosorption for treatment of industrial effluents

Sugarcane bagasse, an abundant agricultural waste from Uganda's sugar industries over 500,000 tons annually are being produced. This serves as a sustainable precursor for biochar adsorbents effective in Pb(II) ions removal (Kumkum & Kumar, 2024). Its surface morphology, oxygen containing functional groups, elemental composition and cation-anion exchange capacity gives it enormous potential to produce biochar as a suitable adsorbent for heavy metal adsorption (Sharma et al., 2024).

Utilising rotten bagasse enhances biochar's adsorption capacity through enriched mineral residues and improved porosity, outperforming fresh bagasse biochar (Bai et al., 2022). Chitosan modification further boosts selectivity and efficiency for Pb(II) remediation by introducing amino and hydroxyl groups for complexation, achieving a higher adsorption capacity as compared to pristine biochar (Bombuwala Dewage et al., 2018)

This approach offers a low-cost and locally viable solution for Uganda's wastewater challenges over a prominent potentially harmful metal, lead.

1.2 PROBLEM STATEMENT

According to the World Health Organisation (WHO), maximum permissible limit of lead in drinking water is 0.05mg/l and for surface water is 0.1mg/L. lead ion concentration in regal paints waste water is above 3mg/L which is a veery high concentration in relation to water quality standards of NEMA of 0.1mg/L. implying this concentration must be reduced before being discharged to water bodies or land surfaces (Sanjay et al., 2021).

The inadequately treated wastewater is deposited in the environment daily posing several health risks such as neurological disorder in children, anaemia and kidney failure in adults. More than 0.6 million of children worldwide suffer from mental retardation annually attributed to blood lead levels (Ranjbar et al., 2023)

Conventional lead removal technologies like chemical precipitation, ion exchange and reverse osmosis are effective but costly, energy-effective and impractical for small scale industries in Uganda and slug disposal associated with some of the methods create secondary pollution problems (Iroegbu et al., 2025)..

Biochar based adsorbents have shown promise for heavy metal removal but many reported materials are either derived from high-cost feedstocks or require complex activation processes that are not easily scalable locally. Raw bagasse biochar's also tend to exhibit limited adsorption capacity and poor selectivity for Pb (II) when compared with rotten bagasse biochar which have an improved porosity and mineral content. Surface modification using chitosan which is a natural biopolymer has been shown to enhance metal ion binding but the use of low-grade agricultural waste such as rotten bagasse as a feedstock for synthesis of biochar for lead (II) removal from real industrial paint wastewater in Uganda has not been adequately explored (Su et al., 2022). Therefore, with the aim of providing an environmentally friendly and economically viable solution for wastewater treatment in Uganda, the project looked at modifying a local feedstock to serve the purpose hence supporting SDG 6 (Clean Water and Sanitation).

1.3 Objectives of the study

1.3.1 Main objective

To develop and evaluate a chitosan modified rotten bagasse derived biochar for selective and efficient removal of lead 2 ions from industrial wastewater

1.3.2 Specific objectives

I. To prepare and characterise a bio adsorbent biochar
II. To obtain the optimal conditions for the adsorption of lead (ii) ions
III. To evaluate the adsorption capacity of a chitosan modified biochar in a paint wastewater

1.3.3 Research questions

1. What are the morphological properties, functional groups and elemental composition of chitosan modified rotten bagasse biochar
2. What are the optimal conditions for maximum removal of lead ii) ions by chitosan modified biochar
3. What are the adsorption mechanisms for chitosan modified biochar

1.3.4 Justification of the study

Lead 2 ions contamination from paint manufacturing sectors in Uganda poses severe health and environmental risks that are exacerbated by inadequate, unsustainable and costly treatment methods (Alharbi, 2023)

Methods like nano-remediation are effective but not eco-friendly since they result into secondary pollutants after their application (Ali et al., 2024). Rotten sugarcane bagasse, ab abundant waste from Uganda's sugar industries can be converted into biochar with enhanced chitosan modification to improve selectivity and efficiency (Bąk et al., 2022)

It utilises local resources to develop a cost effective, sustainable adsorbent, addressing gaps in selective Pb(ii) removal and reusability while supporting SDG 6 (Clean Water) and Uganda's environmental needs

1.3.5 Significance

In accordance to SDG 6 (clean water sanitation), it contributes to improved water quality through the removal of toxic lead from industrial wastewater and reducing contamination of rivers and groundwater used for drinking and agriculture

In accordance to SDG 3(Good health and well-being), it helps to reduce exposure to lead, thus lowering the risk of lead related disease in vulnerable populations

In accordance to SDG 12 (Responsible consumption and production, the project promotes resource efficiency, waste reduction and sustainable industrial practices through the use of locally available biomass and low-cost adsorbents

In accordance to SDF 13 (Climate action) the project utilises agricultural waste instead of burning therefore reducing greenhouse gas emissions and air pollution.

1.3.6 Scope of the study

1.3.6.1 Conceptual scope

The project is directed onto the synthesis of bio-adsorbent composite from rotten sugarcane bagasse, pyrolyse into biochar and then modify with chitosan biopolymer to improve on the porosity and mineral content, expose more oxygen containing groups on the surface of the biochar and to add more functional groups on the surface respectively for maximum adsorption capacity

1.3.6.2 Geographical scope

We collected bagasse from Mayuge sugar limited located in Eastern Uganda and the wastewater from Regal paint limited in Namanve.

(The synthesise of biochar, characterisation and all the experiments were carried out in Nagongera chemistry lab and Busitema materials Lab)

1.3.6.3 Time scope

The time was monitored and limited to only 4 months as in accordance with the Busitema university semester period

1.3.6.4 Conceptual framework

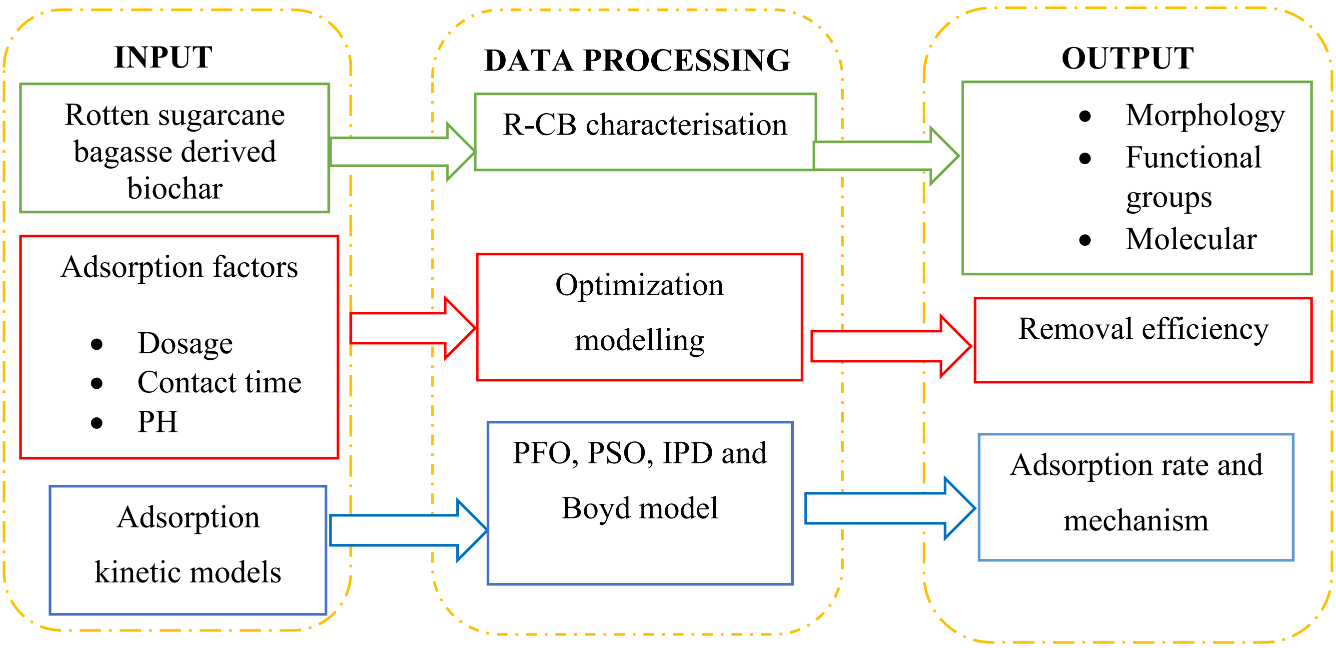

2 CHAPTER TWO: LITERATURE REVIEW

Highlights the increasing concern over lead (ii) ions in water due to their toxic and non-degradable nature, emphasizing the need for effective and eco-friendly removal methods. There are various adsorbents previously used for lead removal but with limitations such as adsorption capacity, stability issues and complex synthesis

2.1 Sources and effect of Lead ions in the environment

Lead element is not found in pure form rather extracted from ores and other minerals by chemical refining processes (R. Zhang et al., 2015). Since it was discovered and used by human for a long time, lead has been widely spreading in the environment. Lead metal get incorporated with water and soils in the environment mainly through anthropogenic activities like mining, smelting and untreated industrial disposals of industrial wastes (Debnath et al., 2019). Though there are natural sources of lead like volcanic explosions and forest fires, but these cause a very insignificant increase in the its concentration in the environment (Zwolak et al., 2019)

Lead enters into the human body main through two ways. Inhalation of lead dust or air at the work place into the respiratory system or digestion of contaminated food and drinks (Charkiewicz & Backstrand, 2020). When it gets into contact with the human body it interferes with every biochemical process by combining with sulfhydryl which causes oxidative stress. It interferes with the functionality of the respiratory system, nervous system in children, kidney and also cardio system causing asthma, lung cancer, brain retardation, kidney failures, heart attack respectively and many other disorders like premature births in pregnant mothers (Raj & Das, 2023)

2.2 Physiochemical properties of paint wastewater

Paints are complex mixtures comprising of organic and non-organic pigments, latexes, extenders, cellulosic and non-cellulosic thickeners and emulsifying agents which with insignificant dilution and treatment, they are responsible for the high concentrations of organic compounds, suspended solids, coloured materials and heavy metals like lead in the generated wastewater (Aniyikaiye et al., 2019). The wastewater is generated from the cleaning of paint manufacturing equipment's like the mixers, reactor, blenders packaging materials and machine and floor.

PH is a very important parameter in wastewater characterisation since almost all chemical reactions in water environment are directly controlled and affected by any change in its value. For paint waste water the PH is found to be in the range of 6.72-7.77 which indicates the alkalinity nature of paint effluents. (Woldeamanuale & Hassen, 2017). Total suspended solids in paint effluents are found to be ranging from 6912.5mg/L to 22528 mg/L showing it is higher than the permissible limit of 100 mg/L due to presence of large number of salts in the effluent.

Due to the presence of large amounts of salt in the effluent, the total suspended solid level goes up to 6912.5mg/L and 22528 mg/L which is extremely higher than the permissible limit (100 mg/L). The toxic substances present in the wastewater can also hike the COD to the range of 425 mg/L to 7662.5 mg/L.

2.3 Sugarcane bagasse as a biomass resource

Sugarcane bagasse is the fibrous residue remaining after juice extraction during sugar production and is abundantly available in the eastern region of Uganda where most of the sugar producing industries are located. Due to its high availability, low cost and environmental concerns, bagasse has attracted attention as a raw material for biochar production (Flávia Rezende Silva et al., 2024). Converting bagasse into biochar not only adds value to this waste but also helps in waste management and mitigation of open burning emissions that contribute to air pollution (Joshi et al., 2023)

2.4 Biochar properties

Biochar is a carbon-rich solid produced through the thermochemical decomposition of organic biomass under oxygen limited conditions, a process known as pyrolysis. It is gaining prominence in environmental remediation due to its physical and chemical properties that effluence its capacity to immobilise contaminants from aqueous solutions.

Structurally, biochar possesses a highly developed internal pore network surrounding micropores, mesopores and macropores. This hierarchical porosity creates a large specific area that often range from tens to several hundred square meters per gram depending on pyrolysis temperature and feedstock composition which provide enough sites for contaminant interaction (Sun et al., 2022). Also, oxygen containing surface functional groups like carboxyl and hydroxyl groups are being preserved and concentrated during carbonisation which severs as active sites for metal ion binding through surface complexation and ion exchange mechanisms.

Biochar is highly resistant to chemical and biological degradation because of its stable aromatic carbon structure it possesses which makes it durable for water treatment. Many articles like (A. Singh et al., 2025) have confirmed the effectiveness of sugarcane bagasse derived biochar as a precursor for reducing dissolved lead concentrations in various experimental conditions

2.5 Effect of natural rotting as a pretreatment for biomass

The use of a pre-decomposed biomass as a biochar precursor represents an emerging and cost-effective strategy for enhancing adsorbent performance. Lignocellulosic materials undergo natural aerobic or anaerobic decomposition; resident microbes enzymatically attack the polysaccharides particularly hemicellulose and portions of cellulose that fill the inter-fibre spaces of the plant matrix. This decomposition removes the space-occupying polymers creating additional porosity within the material hence the resultant bagasse exhibits a rougher, more open surface architecture and greater pore volume. It also mobilises mineral elements on the adsorbent surface like calcium silica and potassium that can participate in ion exchange reactions replacing less strongly bound cations with Pb (II) ions from the solution. (Alokika et al., 2021) & (Mohanty et al., 2024).

Natural microbial pre-treatment avoids the chemical inputs, energy consumption and secondary waste streams associated with chemical activation methods hence matching with the sustainability goals and low-cost adsorbent development (Gayathri & Nair, 2023).

2.6 Modification with chitosan

Chitosan is a linear polysaccharide derived from chitin a structural component of fungal cell walls, mushrooms and arthropod exoskeleton by partial deacetylation process. It has a high dense and reactive functional groups which makes it a good surface modifier for adsorbents, primary amine found on the C-2 position of each glucosamine unit and the secondary and primary hydroxyl groups at the C-3 and C-6 positions respectively act as the electron donors capable of forming stable coordination complexes with soft and broadline Lewis acid metal cations such as Pb(II) ions (Kumar et al., 2025). When impregnated onto biochar surfaces through precipitation from an acetic acid solution using an alkaline cross-linking bath forming a hydrogel-like polymeric coating that covers individual biochar particles. Chitosan coating introduces a high density of additional metal binding sites while largely preserving the underlying pore architecture of the biochar substrate. Research shows that chitosan modification elevates the adsorption capacity of biochar for lead nearly by 1.3 times compared to unmodified material due to the chelation action of the amine groups and the increased surface are of the adsorbent (Sanjay et al., 2021).

The combination of porous, carbon-rich with the chelating biopolymer chitosan produces a composite adsorbent that benefits from the synergistic interactions between the two components. Biochar provides structural rigidity developed porosity and oxygen containing functional groups while chitosan contributes targeted metal binding functionality improved selectivity and potential for the adsorbent regeneration (Niu et al., 2024)(Latha et al., 2023)

2.7 Methods of removing Lead ions from wastewater

Lead (II) ions being one of the major environmental and public health concern because of being toxic even at its low concentrations and when accumulated in living organisms, regulatory agencies (NEMA, WHO) have set acceptable limits for lead discharged in industrial effluents and that in drinking water which calls for extensive work on how remove lead ions from wastewater. As a result, many technologies have been brought about which have several advantages and limitations.

2.7.1 Chemical precipitation

It works by converting dissolved lead ions into insoluble compounds that can be then separated from water as sludge. Studies show it gives high removal at alkaline pH but the generation of large amounts of sludge cause disposal challenges (M. C. Benalia et al., 2022).

2.7.2 Ion exchange

It’s a technique where lead ions are exchanged with harmless ions on a resin of solid matrix. It achieves a good removal efficiency with low-concentration wastewater by its high sensitivity to fouling and costs limit large scale application (Jasim & Ajjam, 2024).

2.7.3 Reverse osmosis

This s a membrane separation process that forces water or wastewater through a semipermeable membrane under pressure, rejecting dissolved ions such as Pb (II) ions from passing through it. RO is considered one of the most efficient methods for lead removal because its membrane can retain very small dissolved ions and produce high quality permeate (Sanjay et al., 2021). The process works mainly through size exclusion and charge effects across the membrane surface, making it very useful when very low final lead levels are required. It's noted that due to the need for high pressure, membrane replacement, cleaning, energy input, and production of concentrate stream that must be further managed, this process becomes relatively expensive limiting its applicability in developing countries like Uganda (Venzke et al., 2017)

2.7.4 Coagulation

This process involves destabilising suspended and dissolved lead ions using coagulants like alum, ferric chloride and lime to neutralise particle charges so that they can form large flocs that settle out or are filtered more easily (A. Benalia et al., 2024).

2.7.5 Electrochemical reduction

This is a process that combines ion transport and electrochemical conversion in one system that removes lead ions by applying an electric current so that dissolved lead ions are converted into a less soluble form or deposited at the electrode surface (Vo et al., 2016). It achieves high removal efficiency in a relatively short time under optimised conditions but its significantly costly because it requires electricity, controlled operating conditions and electrode maintenance rendering it inapplicable in small scale and resource constrained areas(Y. Liu et al., 2013).

2.7.6 Adsorption

Among the available approaches, adsorption has the greatest attention in recent years because of its simplicity and capability to use locally, readily available and low-cost natural materials like agricultural wastes, natural clays, activated carbon and other (Chowdhury et al., 2022). These adsorbents can be engineered by modifying their surface area, pore structure and embedded functional groups to increase their lead ions removal efficiencies from moderate to nearly or complete removal depending on pH, adsorbent dosage, contact time and initial lead concentration (Thompson et al., 2020).

2.8 Adsorption mechanisms

Lead (ii) ions adsorption onto chitosan modified biochar occurs via multiple mechanisms including ion exchange, surface complexation, electrostatic attraction and physical adsorption (Verma et al., 2025). The modification enhances surface chare density, increasing the number of active sites available for lead 2 ions binding. Adsorption isotherms typically follow Langmuir, Freundlich models with adsorption kinetics often fitting pseudo second order models indicating chemisorption dominance (Choudhary et al., 2025).

Research shows that parameters such as pH, contact time, adsorbent dosage and initial metal concentration critically influence lead 2 ions adsorption efficiency (Wanyonyi et al., 2024). Adsorption studies on chitosan modified biochar recommend detailed optimisation for practical applications in wastewater treatment (V. Singh et al., 2024)

2.9 Characterisation of modified rotten bagasse biochar

Characterisation is an important aspect in research were the investigation on the reasons for the behaviour of the product is done. The modified rotten bagasse biochar can be characterised to observe the morphology, surface chemistry, elemental composition and crystallinity which directly affect its effectiveness during adsorption.

SEM-EDX, FTIR and XRD are qualitative and semi qualitative analytical techniques that are used to do characterisation of substances in terms of particle-size distribution, size and mineral content, functional groups and element content respectively (El-Zahhar et al., 2021). These were used to characterise the pristine sugarcane bagasse biochar and the chitosan modified composite before and after Lead (ii) ions adsorption

2.9.1 SEM-EDX

SEM-EDX is a powerful technique that simultaneously provides high-resolution surface morphology imaging and qualitative elemental analysis of the adsorbent. It can be used to confirm the successful modification of biochar and verify the adsorption of heavy metals.

Several studies have reported that raw and rotten sugarcane bagasse biochar exhibits a highly porous, irregular and fibrous morphology with tubular structures originating from the vascular bundles of the bagasse. The rotting process further increases on the surface roughness, creates more cracks and pores hence exposing additional active sites due to microbial degradation of cellulose and hemicellulose.

Chitosan modification shows a smoother surface texture or a thin polymeric covering the biochar particles which appear partially blocking some mesopores yet the overall porous structure is largely retained.

The EDX component is particularly important in confirming the chemical modification and metal uptake. Raw rotten bagasse biochar is predominantly composed of carbon and oxygen with smaller amounts of silica, potassium, calcium and magnesium originating from the high ash content of bagasse due to degradation. After chitosan, a new nitrogen peak appears in the EDX spectrum confirming the successful incorporation of chitosan's amino groups onto the biochar surface.

Following Pb^{2+} adsorption, the EDX spectrum shows a distinct lead peak and elemental mapping often reveal the uniform distribution of Pb on the adsorbent surface. The increase in Pb weight percentage and corresponding decrease in the intensity of other cations e.g. Ca^{2+}, Mg^{2+}, K^{+} provide strong evidence of ion-exchange and surface complexation mechanisms (Malool et al., 2021)

2.9.2 FTIR

FTIR spectroscopy is widely used to identify the functional groups present on the adsorbent surface and to confirm successful chemical modification. Raw sugarcane bagasse biochar generally shows characteristic peaks for O-H stretching (3400-3500 cm^{-1}), C=O stretching of carboxyl groups (1600-1700 cm^{-1}) and Si-O vibrations (around 1000-1100 cm^{-1}) due to the high silica content in bagasse (Akl & Serage, 2024).

In chitosan modified biochar, new or intensified peaks appear at approximately 1650 cm^{-1} (N-H bending of amide I) and 1550 cm^{-1} (N-H bending of amide II), confirming the successful incorporation of chitosan's amino groups ($-NH_2$). The broad O-H and N-H stretching band

(3200-3500 cm^{-1}) also becomes more intense, indicating additional hydroxyl and amino groups available for metal binding.

After lead adsorption, noticeable shifts or reductions in the intensity of -OH, -COOH, and NH_2 peaks are observed. These shifts provide strong evidence of chemical interactions i.e. complexation and ion exchange between lead ions and functional groups on the chitosan modified biochar surface (Manyatshe et al., 2022)

2.10 Response surface methodology

Response surface methodology is a collection of statistical and mathematical techniques designed to model and optimise systems in which a response of interest is simultaneously influenced by multiple independent variables. For the case of adsorption studies, RSM structures a rigorous framework for investigating how process variables such as adsorbent dosage, pH and contact time interact to determine the overall efficiency of the target contaminant.

The principle of RSM designs empirical polynomial model that is typically a second order quadratic to the experimental data collected at systematically varied factor combinations. By capturing the individual, pairwise interactions and curvature effects of variables, this model enables the identification of optimal operating conditions without the need for exhaustive one variable at a time experimentation.

Box Behnken Design is the more suitable experimental design for adsorption studies since for it unlike CCD requires only three levels per factor (-1, 0, +1) and avoid extreme corner points that could produce unstable experimental outcomes. Because of these outstanding features, it has been widely adopted by many researchers' studying optimisation of biochar-based adsorption of heavy metals.

The quality of the fitted RSM model is evaluated through analysis of variance (ANOVA) which partitions the total variation in the experimental response into contributions from the model, individual terms and residual error. Key statistical indicators include F-value and corresponding p-value of the overall model with significant threshold typically set at $p< 0.05$, the coefficient of determination R^2 expressing the proportion of response variability explained by the model, the lack of fit test which assesses whether the model adequately represents the experimental data without systematic error. Three-dimensional response surface plots and contour diagrams generated from the fitted model provide visual representations of the factor-response relationships and interactions which enables intuitive identification of optimum regions within the experimental space.

2.11 Residual analysis.

Response surface methodology is a powerful statistical framework that has been widely used in adsorption studies for simultaneously optimising multiple process variables and modelling their interactive effects on a target response i.e. efficiency. However, the reliability and validity of the RSM model and its optimisation results generated are importantly contingent on the satisfaction of the statistical assumptions that underpin the least-squares regression approach used to fit the model. The systematic examination of the relations between model predicted and experimentally observed response values i.e. Residual analysis is used to as the diagnostic tool to verify these assumptions after model fitting.

2.11.1 Predicted versus actual plot

This plot gives a direct visual assessment of how well the fitted RSM model reproduces the experimental data by plotting predicted response against the corresponding observed values. When the model's fit is adequate, the data points cluster tightly along the 45-degree diagonal without a systematic deviation. Various studies on heavy metal remediation using RSM have employed this plot to visually confirm the observed high R^2 values like (Tigalana et al., 2025) reported a very corelation of predicted and actual Pb (II) removal values along the diagonal for a KOH modified rice straw biochar system that corresponding to the R^2 value of 0.98 reported from ANOVA.

2.11.2 Normal probability plot of residuals

This is the standard plot for assessing the normality assumption in regression models being plotted studentised residuals against their corresponding theoretically expected positions under a normal distribution. If the residuals are normally distributed, the data points align closely along a straight diagonal line. Deviating from the reference line forming a S-shaped curvature indicating skewness or heavy tails indicating kurtosis, is a signal that violates normality and would invalidate F-test and t-test statistics derived from the model. In the adsorption studies, approximately normal residual distributions have been consistently reported for well-fitted RSM models (Akl & Serage, 2024).

2.11.3 Residual versus predicted values plot

The assumption that the variance of model errors is constant across the range of predicted response values known as homoscedasticity, is assessed using this plot. Heteroscedasticity, manifesting as a systematic funnel shape in this plot indicates that the error variance increases and decreases with the predicted value, a condition that undermines the efficiency of ordinary least-squares estimators and can distort significance testing. Most studies report consistent demonstration of homoscedastic residual patterns (Yahya & Elshaarawy, 2024).

2.11.4 Cook's distance plot

Cook's distance is a composite influence measure that quantifies the effect of deleting a single observation on the entire set of fitted regression coefficients simultaneously. An observation with a cook's distance exceeding 1 is conventionally identified as potentially influential and warranting investigation as its removal could substantially alter the model's parameter estimates and predictions. The importance of checking cook's distance in adsorption PSM studies has been highlighted by several authors. (Chowdhury et al., 2022) reported that influential observations in BBD datasets for heavy metal adsorption frequently arise from runs conducted at extreme combinations of factor levels where experimental variability tends to be higher. In well-executed adsorption experiments with consistent laboratory protocols and properly calibrated instruments, Cook's distances are typically well below the threshold of 1 indicating that the model is robust and that all experimental observations contribute proportionally to the regression without undue leverage.

2.11.5 Residuals versus run order plot

This plot is used to detect violations of the independence assumption. The presence of systematic trends, autocorrelation or time dependent patterns in the model errors that would indicate that successive experimental observations are not statically independent of one another due to instrument drift, reagent degradation and changes in environmental conditions like temperature. When residuals are genuinely independent, this lot should sow a random, unsystematic scatter around zero with no directional trend or cyclic behaviour.

2.11.6 Box-cox plot

The Box-cox power transformation procedure provides a data driven method for identifying whether and how the response variable should be mathematically transformed to better satisfy the normality and homoscedasticity assumptions of the regression model. The procedure evaluates a family of power transformations parameterised by lambda, ranging from negative reciprocal transformations through logarithmic (lambda = 0) and square root (lambda = 0.5) to no transformation (lambda = 1), and identifies the lambda value that minimises the residual sum of squares. The 95% confidence interval for the optimal lambda is visualised graphically; if this interval includes lambda = 1, no transformation is required. In adsorption percentage removal studies, the response variable is inherently bounded between 0 and 100%, which can sometimes introduce mild non-normality at extreme values. However, across the majority of published biochar adsorption RSM studies, lambda values close to 1 have been reported, indicating that percentage removal data satisfies regression assumptions without transformation when the experimental design is well-constructed and the response range is not excessively narrow or concentrated near the bounds

2.12 Adsorption kinetics

Adsorption kinetics describes the time dependent evolution of the adsorption process by demonstrating how rapid and by which mechanism the adsorbate particles are moved from the solution to bind on the adsorbent surface. This analysis reveals the rate controlling steps that govern the efficiency of the adsorbent under favourable conditions.to preserve the statistical integrity of the original experimental data it’s advisable to use non-linearised fit kinetic models (Foo & Hameed, 2010)

The pseudo first order (PFO) also known as the Lagergren model assumes that the rate of adsorption is proportional to the difference between the equilibrium adsorption capacity and the instantaneous capacity at time (t). it reveals physisorption, a physical interaction between the adsorbate and adsorbent. The pseudo second order (PSO) assumes that the rate of adsorption is proportional to the square of the remaining unoccupied active sites on the adsorbent surface. The model reveals the adsorption involving the formation of chemical bonds a process called chemisorption. Its specially gives the estimate of the equilibrium adsorption capacity and the initial adsorption rate of the adsorption process (Revellame et al., 2020).

The intraparticle diffusion model (IPD) examines the transport of adsorbate molecules through the pore network of the adsorbent particle after initial surface attachment. If the plot goes through the origin, it means the intraparticle diffusion is identified as the sole rate-controlling mechanism for the adsorption process. The Boyd model is always employed to differentiate between the two principal external and internal rates controlling mechanisms i.e. the film diffusion that involves ass transfer of adsorbate through the boundary layer surrounding each adsorbent particle and intraparticle diffusion. When the Boyd plot is linear and passes through the origin, pore diffusion is rate-controlling mechanism well as if it's a positive intercept, it assumes that film diffusion governs the initial rate.

3 CHAPTER THREE: METHODOLOGY

This chapter describes the analytical and experimental techniques used to study Pb (II) ions removal from industrial paint wastewater. Carbonisation and modification of fresh and rotten sugarcane bagasse, characterisation of the adsorbents and wastewater, batch adsorption experiments, adsorption optimisation and adsorption kinetics experimental designs were carried out under controlled laboratory circumstances to produce accurate evaluation of adsorption performance of the adsorbent on Pb (II) ions.

3.1 Preparation and modification of fresh and rotten bagasse biochar

Sugarcane bagasse was collected from Mayuge sugar limited and stored in an air tight package to undergo anaerobic biodegradation for 2 months (Mukunda et al., 2025) which caused lignin structure break down and increase in mineral residual and oxygen containing groups in the bagasse. The rotten bagasse was dried under sun light for 24 hours and then carbonised using a biochar kiln forming a rotten bagasse biochar (RBB). It was crushed and sieved to a uniform 0.5mm size and then washed to remove impurities. The wet RBB was oven dried under the temperature of 70°C for 12hours (Akl & Serage, 2024)

As reported by (Bombuwala Dewage et al., 2018) using a ratio of 1:3, 7g of chitosan was dissolved in 520ml of Acetic acid (2%) followed by addition of 21g of rotten bagasse biochar with vigorous stirring for 6hr using an orbital shaker (Stuart SSL 1). Then the chitosan-biochar suspension was added drop wise into a 2100ml of sodium hydroxide (1.2%) and the resulting suspension held for 12hours (Akl & Serage, 2024).

The solution was filtered through doubled Whatman no.1 filter paper with a suction machine and then washed with deionised water to remove excess sodium hydroxide and oven-dried for 24hour at 70°C hence bio-adsorbent CH-RBB (chitosan modified rotten bagasse biochar).

3.2 Characterisation of FBB, RBB, CH-FBB and CH-RBB

A Fourier transforms Infra-red spectroscopy (FT/IR-6600 type A) by taking scan at $4000cm^{-1}$ and $400cm^{-1}$ at a resolution of $16cm^{-1}$ to obtain the functional groups on the structure of the rotten bagasse biochar. A VEGA3 TESCAN Scanning Electron Microscope was used to ascertain the morphological properties of the biochar's surface by using operated at an accelerating voltage of 10.0kV using a secondary electron detector, working distance of 15.00mm magnification of 1,000×. (Amin et al., 2016; Loc et al., 2022)

3.3 Collection and characterisation of paint wastewater

By grab sampling as directed by U.S federal regulations guidelines establishing test procedures for the analysis of pollutants (40 CFR part 136), paint wastewater was collected from regal paints Uganda limited using a 5 litre plastics jerrycan which was washed with nitric acid before putting the water to prevent Lead ions from reacting on the walls of the jerrycan (Stark et al., 2015).

It was then analysed to know the concentration of Lead (II) ions and levels of the influential factors that affects adsorption i.e. pH, total dissolved solids, total suspended solids, electro conductivity, chemical (Wojnárovits et al., 2024). All were down following standard protocol for water and wastewater examination.(Adams, 2017).

The pH of the effluent was ascertained using a Ex Stick EC500 pH meter by immersing a meter robe in a 50ml beaker with wastewater when the pH meter is switch on, it was left to settle for a few seconds and then read the stable value of the pH displayed. The Lead (II) ions concentration was analysed using JENWAY 6705 UV Vis's spectrophotometer by KI-CPE method. This was done by adding a few drops of KI in 2ml of wastewater and then added acetate buffer followed by a surfactant (polysorbate 80) and heat the mixture in a water bath at 50℃ for 10 minutes. Then centrifuged at 4000rpm for 5 minutes using an Omega 6 centrifuge machine and solidified the surfactant by cooling in an ice bath for 2 minutes which was later extracted to a cuvette and diluted using ethanol. Its absorbance was then measured at $420nm^{-1}$(Hussain et al., 2024).

To evidence the presence of anions and cations in the effluent, the levels of electrical conductivity and total dissolved solids were analysed using the Ex Stik EC500 meter. It was done by submerging the meter robe into a 250ml beaker with the wastewater and the readings taken from the display (Yirdaw, 2025). And COD was measured using HI9146 Dissolved Oxygen Meter.

3.4 Batch experiments

Batch experiments were carried out on this real paint wastewater with investigation factors being CH-RBB adsorbent dosage (A: 0.1-2g), pH(B: 3-8) and contact time(C: 15-80min) with response surface methodology with Box Behnken Design (RSM-BBD) in design expert 13 software to design the batch experiment generating an empirical model and optimise the factors for lead (II) ions adsorption (Tigalana et al., 2025).

Table 3.1: Independent variables for Design of experiment

Factor	Name	Units	Minimum	Maximum	Coded Low	Coded High
A	Adsorbent dosage	g	0.1000	2.00	-1↔ 0.10	+1 ↔ 2.00
B	pH		3.00	8.00	-1↔ 3.00	+1 ↔ 8.00
C	Contact time	minutes	15.00	80.00	-1↔15.00	+1 ↔ 80.00

Using the model, the adsorption process was optimised and the optimised values were used to investigate the removal efficiency of lead ions using the modified fresh bagasse biochar. Evaluated the significance of the model using ANOVA, individual factors and interaction effects on the process of adsorption

3.4.1 Adsorption process

Following the BBD the samples of 50ml of wastewater was put in 250ml conical flasks, adjusting the pH using 0.1mol/L nitric acid and 0.1mol/L sodium hydroxide with the use of a pH meter (Bombuwala Dewage et al., 2018). Using the analytical balance, the required grams of the adsorbent was measured per run then the mixture was shaken using an orbital shaker at 200rpm at room. After sorption, the suspensions were filtered using Whatman no.1 filter papers to prevent traces of adsorbent from going with the filtrate, two layers of the filter papers were used.

3.4.2 Measuring concentration of lead (ii) ions at equilibrium

Using potassium iodide as a reagent for complexing the lead ions from the filtrate, a Cloud point extraction method was used to measure the concentration of lead(II) ions that remained in the filtrate with a 6705 JENWAY UV Vis's spectrophotometer (Hussain et al., 2024).This was done by first obtaining the standard curve of absorbance versus concentration in excel office and then used it to get the unknown concentrations.

The amount of Lead (ii) ions to be adsorbed per unit mass of the adsorbent (Q_e) calculated from the mass balance equation

$$Q_e = \frac{(C_o - C_e)V}{m}$$

Equation 3.1

Where Co and Ce are the initial and the equilibrium concentrations of Pb^{2+} respectively, V is the volume of the solution in litres, m is the weight of the biochar, Qe is the amount of Pb^{2+} adsorbed per unit mass (mg/g).

The removal percentage of Pb^{2+} is to be calculated as

$$Removal\ efficiency(\%) = \frac{C_o - C_e}{C_o} \times 100$$

Equation 3.2

To assess the statistical significance of model terms and evaluate the relative contribution of each independent variable of Pb^{2+} removal efficiency, the experimental data will be subjected to ANOVA at a 5% significancy level.

3.5 Adsorption rate of Pb (II) on to CH-RBB

The adsorption rate of Lead(II) ions on to chitosan modified sugarcane bagasse biochar was evaluated using pseudo first and second order models, intraparticle diffusion model and Boyd models non linearly Plotted on one axis using Origin pro-2018 software (Burk et al., 2020)

Pseudo first order model directly estimated the equilibrium capacity (represents physisorption) and Pseudo second order used to determine whether the rate of adsorption is proportional to the square of the number of unoccupied sites (representing chemisorption) and gave a direct estimate of adsorption capacity. The intraparticle diffusion model (Weber-Morris model) determined how adsorbate molecules move inside the pores of an adsorbent particle and the rate-controlling step during adsorption. The Boyd graph differentiated between external boundary layer diffusion (film diffusion) and the intraparticle diffusion as the dominant mechanism controlling adsorption rate

Table 3.2: Nonlinear equations for adsorption kinetic model

Kinetic models	Integrated Equations
PFO	$q_t = q_e(1 - e^{-k_1 t})$
PSO	$q_t = \frac{{q_e}^2 k_2 t}{1 + q_e k_2 t}$
IPD	$q_t = k_{id} t^{\frac{1}{2}} + C$
Boyd graph	$B_t = -0.4977 - \ln(1 - F), F = \frac{q_t}{q_e}$

4 CHAPTER FOUR: RESULTS AND DISCUSSION

The experimental results on the modification and removal of Pb (II) ions from paint wastewater using chitosan modified rotten bagasse biochar are reported and explained in this chapter. In order to explain removal efficiency, underlying mechanisms and practical applicability, the outcomes of modified biochar characterisation, process optimisation and adsorption modelling are assessed.

4.1 Biochar characterisation

4.1.1 Surface structure of rotten and modified and loaded biochar.

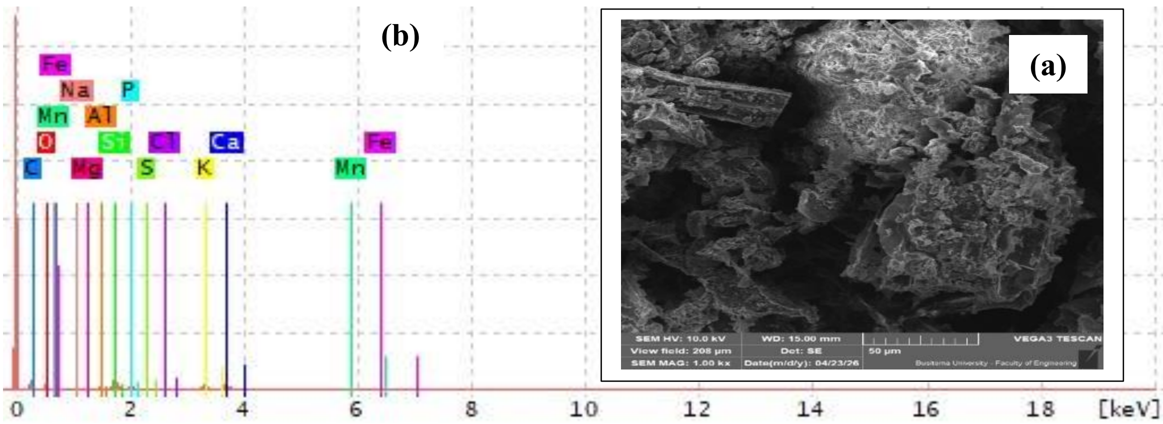

Figure 4.1: SEM image for RBB (a), EDX graph for RBB (b)

Pristine RBB (figure 4.1 a) surface is largely dominated by large, irregularly shaped, massive agglomerates with rough and highly textured faces. The central field shows a prominent, rounded and granular agglomerate covered with a dense irregular microrough coating, a morphology consistent with the partial pre-decomposition of the bagasse feedstock by microbial degradation prior to pyrolysis (Mastalerz et al., 2023). Microbial decomposition in rotten bagasse preferentially degrades hemicellulose and cellulose which disrupts the ordered fibrous vascular structure and leaving a disordered carbon matrix after pyrolysis. The presence of prismatic crystal-like structures in the upper-left field corresponds mineral residues mobilised during the decomposition process (Emenike et al., 2026).

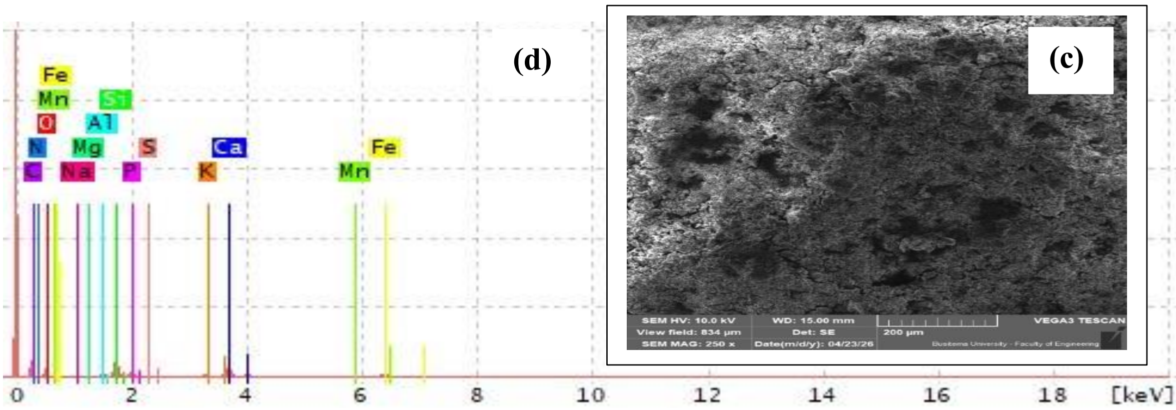

Figure 4.2: SEM image for Chitosan rotten bagasse biochar (c), EDX image Ch-RBB (c), EDX image for Ch-RBB (d)

In figure 4.2(c) the micrograph reveals a more compact and homogeneous surface structure. This agglomerate presents a rough, granular face covered with a fine, uniformly distributed particulate coating, a morphological suggesting chitosan polymer deposition onto the biochar substrate. This is consistent with the crosslinking and precipitation of chitosan chains onto biochar particle surfaces during the modification process (Salam et al., 2012). This chitosan surface modification forms a thin hydrogel-like polymer film on the biochar surface upon drying, covering individual particles and introducing a high density of aminol and hydroxyl functional groups available for metal ion coordination (Li et al., 2022) .

Compared to pristine RBB, Ch-RBB shows a marked reduction in the visibility and apparent volume of macropores. The large open void channels prominent in the RBB micrograph are substantially occluded in Ch-RBB as the chitosan film bridges across inter particle pore openings and fills shallow surface crevices. While this pore occlusion reduces the overall macropore volume, it simultaneously increases the mesopore surface are by creating a new, chitosan surface layer over the biochar framework (Inyang et al., 2016). The net effect is a redistribution of pore size distribution from macroscope dominated in RBB towards a greater contribution of mesopores in Ch-RBB which is more favourable for heavy metal adsorption as mesopores provide higher surface are per unit volume for metal ion functional group interactions (Ezeonuegbu et al., 2021)

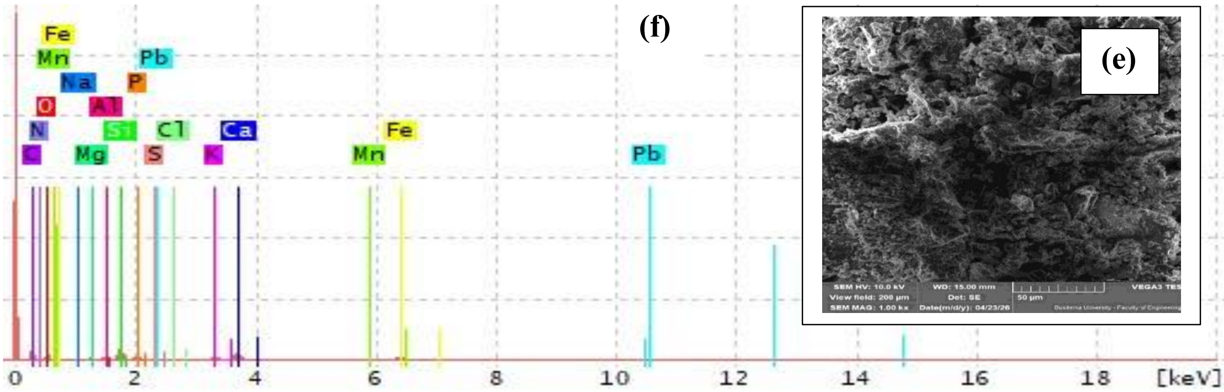

Figure 4.3: SEM image for Pb-Ch-RBB (e), EDX image for Pb-Ch-RBB (f)

Figure 4.3 (e) reveals a pronounced three dimensional, highly porous surface architecture with significant topographic relief. The multiple structure motifs consist of angular plate-like fragments, elongated fibrous structures and rounded nodular clusters all uniformly coated with a fine nano scale particulate deposit. This nano textured coating absent in Ch-RBB is attributed to the precipitation of lead hydroxide and lead carbonate micro-crystals on the chitosan biochar surface following Pb^{2+} uptake (He et al., 2010). These observations confirm chemisorption as one of the mechanisms involved in Pb^{2+} adsorption.

The EDX observations aligns with the SEM discoveries. In figure 4.1 (b) there is an observed large number and high %age composition of mineral elements i.e. K, Ca, Mg, Si and others due to specifically pre-decomposition of bagasse prior to pyrolysis. The presence of N(NH_2) and increase in O(-OH) percentage composition from 30.4% to 31.1% in Figure 4.2 (d) confirms the configuration of chitosan biopolymer onto the biochar. And after adsorption the peak for Pb metal was observed in figure 4.3 (f) which was absent in the other EDX graphs confirming the binding of Pb (II) ions on to the functional groups of the adsorbent through complexation. A significant reduction in the percentage composition of some mineral elements supported ion exchange process during Pb (II) ions remediation i.e. K (4.8% to 0.9%), Si (9.9% to 9%) and Ca (7% to 6.2%).

4.1.2 Surface functional groups of biochar

Figure 4.4 shows the FTIR spectrum comparing surface functional groups of pristine RBB, modified RBB before and after loading. The spectrum shows change in wave number and intensity of some peaks suggesting the inclusion of surface functional groups in the adsorption of Lead (II) ions through complexation.

A broad and prominent band observed between 3363cm^{-1} and 3580cm^{-1} is attributed to the overlapping stretching vibrations of ^{-}OH and $^{-}NH_2$. Its intensity increased markedly in Ch-RBB confirming the successful grafting of chitosan which is rich in $^{-}NH_2$ and ^{-}OH and a broad and prominent band observed between 3363cm^{-1} and 3580cm^{-1} is attributed to the overlapping stretching vibrations of ^{-}OH and $^{-}NH_2$ (Divband Hafshejani et al., 2016). Its intensity increased markedly in Ch-RBB confirming the successful grafting of chitosan which is rich in $^{-}NH_2$ and ^{-}OH. After Pb^{2+} adsorption, there was observed decrease in the intensity of this band which means hydroxyl and amino groups interacted with Pb (II) ions forming complexes (C. Zhang et al., 2025).

The observed slight shift of carboxylate group (^{-}COO) from 1590cm^{-1}in Ch-RBB to 1565cm^{-1} in Pb-Ch-RBB indicates complex formation between Pb^{2+} and ^{-}COO forming Pb-COO confirming adsorption via chemisorption (Poonam & Kumar, 2020). C-N groups with positive charge are responsible for the peak observed at 1400cm^{-1} in Ch-RBB and shifted to 1369cm^{-1} in Pb-Ch-RBB justifying its involvement in adsorption (Luo et al., 2014)

The spectrum region below 700cm^{-1} exhibit a strong band in all the samples due to the presence of mineral elements as a result of pre-decomposition prior to pyrolysis (Xie et al., 2022) but its highly intense and significant after adsorption suggesting additional vibration of Pb-O which arise from inner sphere Pb^{2+} complexes on the sorbent surface (Zhao et al., 2021).

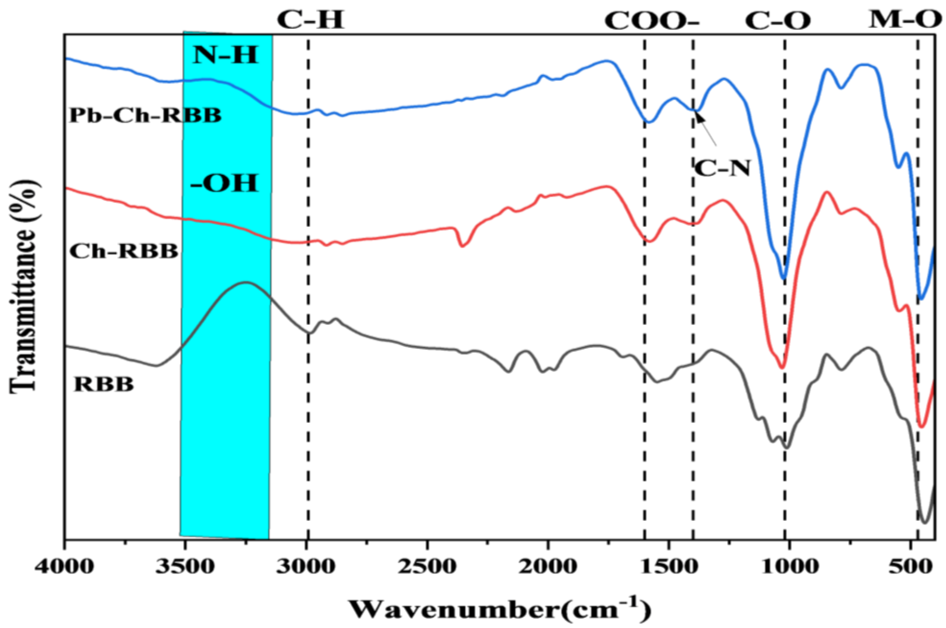

Figure 4.4: FT/IR graph showing functional groups on RBB, Ch-RBB and Pb-Ch-RBB

4.2 Paint wastewater Characterisation

The Ph value of the effluent was recorded as 6.60 suggesting a slightly neutral nature of the effluent which aligns with the WHO's acceptable range of 6-9 in discharged water and NEMA standard of 5.5-8.5. its Electrical conductivity was found to be 13543µS/cm which was slightly above that of the permissible limit for national environment ministry (EC < 1000µS/cm) but below limits for NEMA of 1500µS/cm. These were measured using EC500 Ex Stik II.

The COD is an indicator of pollution level in the industrial effluents and it was found to be 153mg/L surpassing both the WHO's limits (120mg/L) and NEMA (100mg/L) in discharged water.

The concentration of lead ions was found to be 3.88mg/L which is low according to findings in other researches but significantly higher that the permissible limit for NEMA of 0.1mg/L for discharged water on land and that of WHO (0.01mg/L) for drinking water.

4.3 Modelling and optimisation

4.3.1 Response surface methodology -BBD

Using design expert software, BBD was used to an empirical design value for the variables which were considered to run the experiments and removal efficiency obtained as below;

Table 4.1: Removal efficiency of Pb (II) ions under various conditions

Run	Factors			Removal efficiency (%)
	A	B	C	
1	2	5.5	80	85
2	1.05	8	15	80
3	1.05	5.5	47.5	96
4	1.05	5.5	47.5	94
5	1.05	3	15	89
6	1.05	5.5	47.5	99
7	1.05	3	80	79
8	0.1	3	47.5	79
9	0.1	5.5	15	87
10	1.05	8	80	82
11	2	5.5	15	87
12	0.1	5.5	80	81
13	0.1	8	47.5	74
14	2	3	47.5	79
15	2	8	47.5	77

$$R.E(\%) = 96.33 - 1.63B - 2C + 3BC - 8.2A^2 - 10.79B^2 - 3.04C^2$$

Equation 4.1

4.3.2 Analysis of variables (ANOVA)

Significancy of the model and individual terms was analysed using ANOVA at 5% significancy level. The model was very significant with F=38.82, $P < 0.0001$ and a high coefficient of determination ($R^2 = 0.9573$) which shows that 95.7% of the variability in Pb (II) removal efficiency was sufficiently explained by the model. Significant individual factors: pH(B), contact time (C), interaction terms: BC and quadratic terms being A^2, B^2 and C^2.

Table 4.2: **ANOVA for Reduced Quadratic model**

Source	Sum of Squares	df	Mean Square	F-value	p-value	
Model	736.44	6	122.74	38.82	< 0.0001	significant
B-pH	21.13	1	21.13	6.68	0.0324	
C-Contact time	32.00	1	32.00	10.12	0.0130	
BC	36.00	1	36.00	11.39	0.0097	
A^2	253.85	1	253.85	80.30	< 0.0001	
B^2	430.01	1	430.01	136.02	< 0.0001	
C^2	34.16	1	34.16	10.81	0.0111	
Residual	25.29	8	3.16			
Lack of Fit	12.63	6	2.10	0.3322	0.8756	not significant
Pure Error	12.67	2	6.33			
Cor Total	761.73	14				

To improve model predictive robustness, model reduction was performed by excluding statistically insignificant terms ($p > 0.05$) from the full quadratic model and that is A, $p = 0.1842$, AB, $p = 0.3935$ and AC, $p = 0.2685$. The model only retains significant terms, improved adjusted R^2 and predicted R^2 alignment indicating better generalisability and predictive accuracy.

4.3.3 Residual analysis

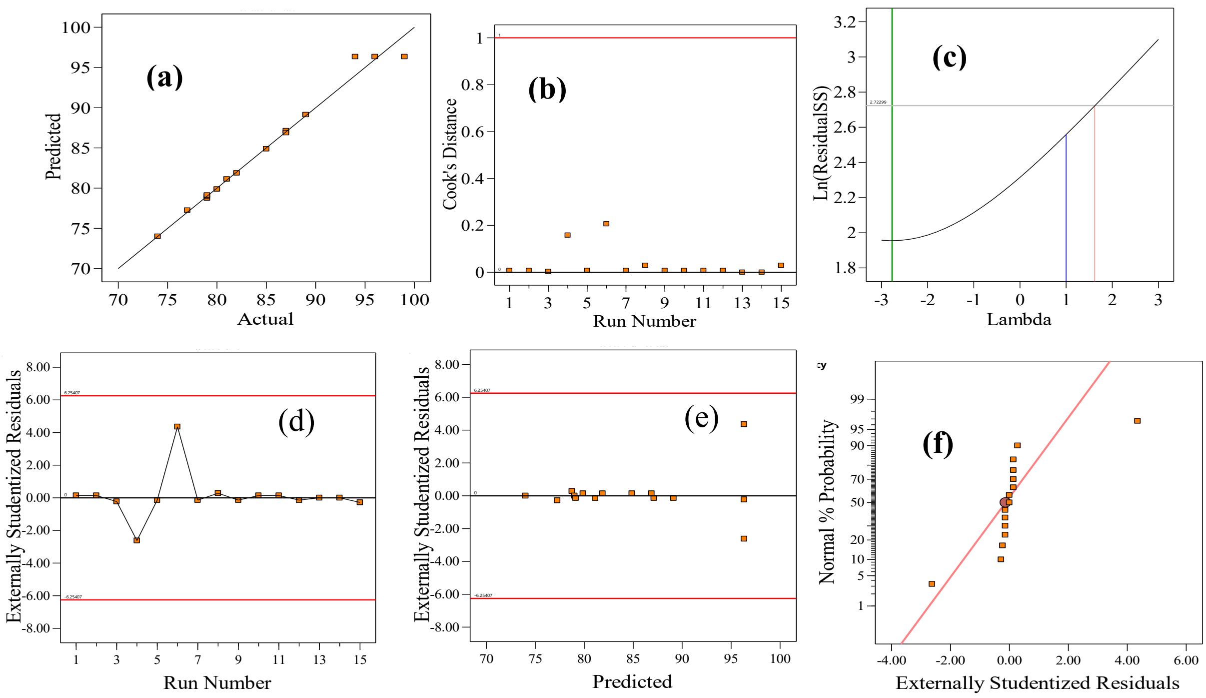

Figure 4.5: Residual analysis for RSM-BBD model;(a) predicted vs actual removal efficiency, (b) cook's distance plot, (c) Box-cox plot, (d) Residuals vs run number, (e) Residuals vs predicted removal efficiency, (f) Normal probability plot.

Figure 4.3 shows a residual diagnosis of the RSM-BBD quadratic model generated for Pb(II) removal by Ch-RBB to validate and put confidence its adequacy and reliability. The predicted versus actual plot (figure 4.3(a)) clearly shows clustered data points along the 45 degree diagonal referance line across the entire respose range of approximately 74% to 99% with no systematic curvature of deviation from linearity. This alignment confirms that the model accurately captures the relationship between all the experimental variables and the removal response validating the high coefficient of determination reported by ANOVA.

Cook's distance plot in figure 4.3(b), all experimentla runs give cook's distance values very low and below the critical threshold of 1 with most of them even approaching zero. Although run 5 shows the highest cook's distance but it remains far under the threshold which confirms that all observations contribute appropriately and proportionaly to the regression and no single experimental run disproportionately controls the model.

Figure 4.3(c) shows Box-cox plot diplays the sum of squares of residuals as a function of the lambda transformation parameter with the optimal lambda value indicated by the verticle line and the 95% confidence interval bounded by the green and red verticle lines. The plot shows the optimal lambda value falling within the confidence interval that encompasses lambda = 1 suggesting that no transformation of the removal efficiency is required hence confriming that the raw percentage removal data satisfies the variance homoscestacidity and normality assumptions of a linear model without need for mathematical transformations.

Figure 4.3(d) detects systematic trends over the sequence of experiments that might indicate time-dependent effects like operator fatigue, changing laboratory conditions or instrument drift hence identifying potential outlier. The horizontal red lines at ±6 define the outlier threshold. In our plot, all residuals are perfeclty constrained with in these bounds and values spread randomly about the origin with no discernible trend, cyclic pattern or directional drift across the run order confirming that the experimental pattern introduced no systematic error into the dataset and that the model error is purely random.

To check for heteroscedasticity across the range of predicted values, a plot of externally studentised residuals vs predicted values in figure 4.3 (e) is analysed. The plot shows a randomly and systematically distributed residuals about zero horizontal line across full range of predicted values constricting all points within the acceptable studentised residual bounds which confirms homoscedasticity (constant model error variance) hence validating the appropriateness of the ordinary least-squares fitting approach used in the RSM anaysis.

The normal probability plot figure 4.3 (f) shows residual points following the refernce line across the central range of distribution with only minor deviations at the extremes but no skewness nor kurtosis. This satisfactory adherence to normalty confirms that all statistical tests performed on the model ie F-test ($F = 32.2$, $p = 0.0007$) and individual term signficance tests are stastistically valid and reliable.

4.3.4 Optimisation of adsorption conditions

The predicted optimum conditions occurred at adsorbent dosage of 1.65g, solution pH of 6.7, contact time of 80minutes, maximum removal efficiency of 87.4% and equilibrium adsorption capacity of 1.835mg/g. Using the obtained optimal conditions, control experiments were run using pristine rotten bagasse biochar and another one using chitosan modified fresh bagasse biochar achieving an equilibrium adsorption capacity of 1.23mg/g and 1.49mg/g respectively. These results align with those of other researchers (Bai et al., 2022) and (Yahya & Elshaarawy, 2024) showing that chitosan modified biochar always show an increase in the adsorption capacity because of the chelation effect of amino groups that have high affinity for Lead (II) ions which is higher than effect of mineral residues obtained from rotten bagasse.

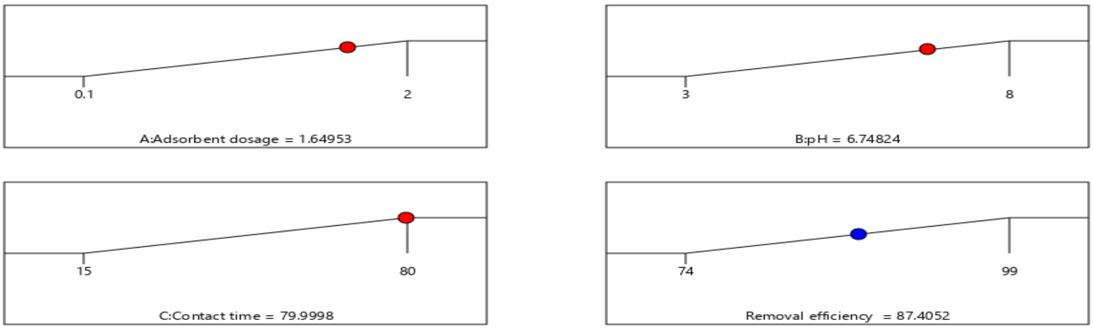

Figure 4.6: Predicted removal values after optimisation

4.3.5 Analysis of variable interactions

The RSM-BBD model generated 3D response surface plots to analyse the combined effects of adsorption variable on Pb (II) ions removal. These plots show the interaction between two factors while keeping the remaining factor constant at their midpoint levels hence understanding the effects of synergistic and antagonistic effects on Pb^{2+} removal.

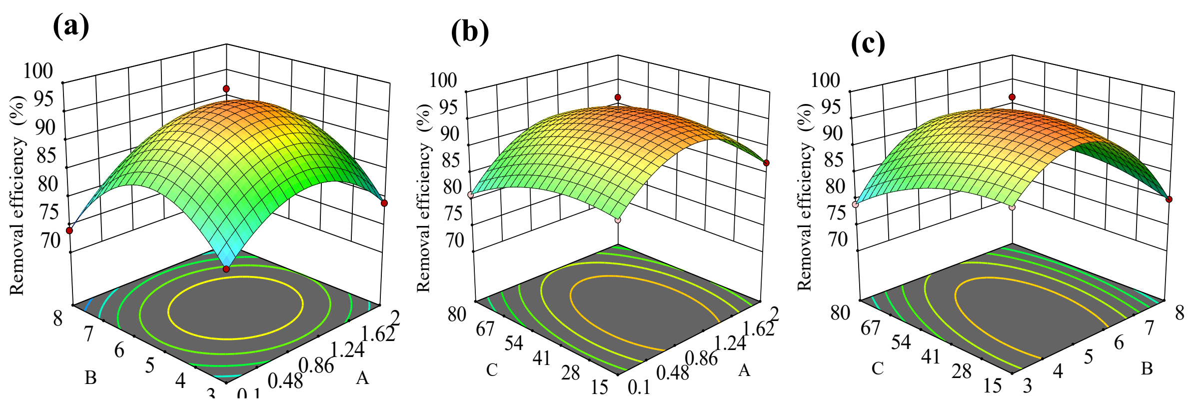

Figure 4.7:Interaction effects of variables on Pb (II) ions removal; (a) AB, (b) AC, (c) BC

Synergic effects were observed in the two-factor interaction ($p < 0.05$) between BC (+3, p = 0.0135) indicating that these two factors combination positively influence Pb (II) removal efficiency. The significant negative quadratic terms A^2(-8.24167, p = 0.0002), B^2 (-10.7917, p < 0.0001) and C^2(-3.04167, p = 0.0150) confirm concave behaviour indicating optimal intermediate factor level. Meaning excess adsorbent dose may cause active site overlap, high pH cause formation of insoluble complexes and longer contact time causes saturation of active sites hence leading to minimal removal efficiency. These interactions suggest that the adsorption process is not additive and the efficiency depends on the optimal balance between multiple factors rather than individual levels alone.

4.3.6 Effect of independent adsorption variables on removal of lead ions

the effect of each factor was demonstrated on box plots describing how each independently effluence Pb (II) ions removal by the adsorbent as shown in the figure below;

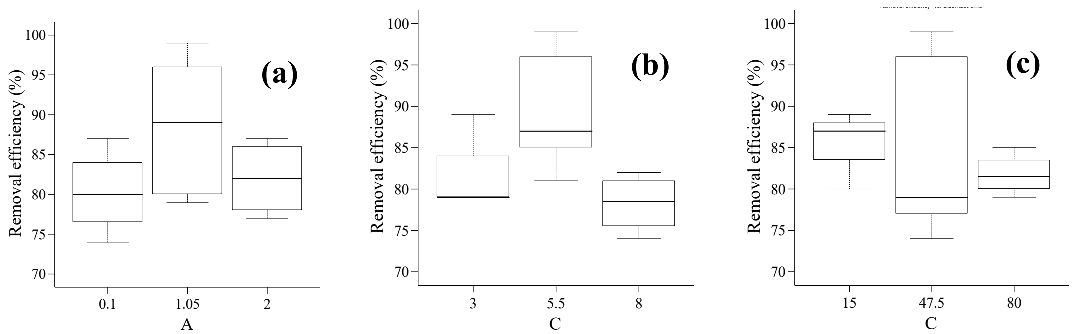

Figure 4.8: One factor effect; (a) R.E Vs A, (b) R.E Vs B, (c) R.E Vs C

4.3.6.1 Adsorbent dose

At the lowest dosage of 0.1g/L, the removal efficiency is relatively low with a median at 80% and a narrow box which indicates low variability. This is due to the insufficient active sites to bind all the Pb^{2+} ions present in solution. At the intermediate dosage, both the median removal efficiency and the spread significantly increased, median rising up to 90%. The wider box indicates greater variability across experimental runs at the dosage reflecting that at moderate dosage levels the system is sensitive to the other factors interacting with it. At the highest dosage of 2g/L, the median removal drops back down to 82% and the box narrows again. This is due to particle aggregation at excess dosage, because the adsorbent particles clump together blocking active sites and reducing the effective surface area available for Pb^{2+} binding

4.3.6.2 PH

At lower pH, the median removal efficiency is moderate at around 82% but shows considerable spread. This is due to the highly acidic environment that causes protonation of the adsorbent's functional groups ($-NH_2$ to $-NH_3^+$) and (-COO- to -COOH), making them positively charged and therefore electrostatically repulsive towards Pb^{2+} ions. At pH 5.5, the highest and most consistent removal efficiencies are recorded, with the median approaching 95% and a relatively wide interquartile range reflecting interaction with other variables. This is because at near neutral pH, the functional groups are deprotonated and freely available for chelation and complexation with Pb2+ ions, making this the optimal pH zone. At pH 8, removal efficiency drops with the median falling to around 78% and narrowing of the box. At high pH, Pb^{2+} begin reacting with excess hydroxy ions to form soluble $Pb(OH)^+$ and insoluble $Pb(OH)_2$ precipitates which have lower affinity for the adsorbent surface.

4.3.6.3 Contact time

At 15 minutes, the median removal efficiency is around 87% with moderate spread. At this early stage, only the easily accessible external surface sites of the adsorbent have been utilised because Pb^{2+} ions have not had sufficient time to diffuse into the internal mesopore and interact with the deeper active sites. At 47.5 minutes the highest removal efficiencies are recorded with the widest interquartile range, suggesting the system is near its adsorption peak but still sensitive to the combined influence of other factors. By this time, Pb^{2+} ions have diffused into the interior pore network and formed strong bonds via electrostatic attraction, surface complexation and ion exchange. At 80minutes, the median removal efficiency decreases slightly and the box becomes very narrow with very low variability. This is attributed to partial desorption of weak bonds of Pb^{2+} with the adsorbent and saturation of the active sites creating a reverse concentration. The narrow box at 80 minutes indicates that the system has reached a stable near equilibrium state where results are highly reproducible regardless of the other factors levels.

4.4 Adsorption kinetic

By employing the optimal values obtained from the optimization process of the RSM-BBD model of A-adsorbent dose of 1.6 , pH of 6.7, Qe of 1.835, experiments where run varying the contact time in the range of 15 to 80 minutes to get the adsorption capacity at a given time (qt) that was used to plot and fit the PFO, PSO, IPD and Boyd model using excel and origin lab.

Table 4.3: Adsorption kinetics constants

PFO model		**PSO model**	
$\boldsymbol{qe(mgg^{-1})}$	1.82	$qe(mgg^{-1})$	2.082
$\boldsymbol{k_1}$	0.074	k_2	0.052
$\boldsymbol{R^2}$	0.971	R^2	0.988
IPD model		**Boyd model**	
$\boldsymbol{k_{id}(mg/gmin^{-0.5})}$	0.1084	$B_t(min^{-1})$	0.082
C	0.9533	R^2	0.957
$\boldsymbol{R^2}$	0.89		

Figure 4.6 (a) shows nonlinear fitting of PFO, PSO and IPD models that describe the kinetic rate and possible mechanism of adsorption of lead ions onto the Ch-RBB. The PSO model gives the best fit of R^2 = 0.988 which means that chemisorption was the dominant rate controlling mechanism since it outweighed PFO (R^2 = 0.971), IPD (R^2 = 0.890) and Boyd (R^2 = 0.957).

PFO assumes that the adsorption rate and directly proportional to the number of vacant sites present. Its curve deviates at mid-point form the experimental data giving a lesser R-squared (R^2 = 0.971) that PSO suggesting that adsorption rate wasn't dependent on physisorption mechanism. PSO suggests the absorption rate is directly proportional to the square root of unoccupied active sites which means two active surfaces are involved in the binding of each Pb^{2+}. The PSO has the best fitting plot with extremely high R^2 value of 0.988 shows excellent linearity suggesting that chemisorption (chemical bonding between Pb^{2+} and the functional groups on the adsorbent) is the dominant and the rate determining mechanism. This confirms the findings from the FTIR results that suggested chemical interaction of Pb^{2+} with surface functions groups of the adsorbent forming complexes.

IPD involves the transportation of Pb^{2+} through the inner pore structure of the adsorbent Intraparticle diffusion plot obtained a good but unreasonable fit with R^2 = 0.89 and noticeable scatter which does not pass through the origin (intercept, C=0.9533) suggesting that intraparticle diffusion is occurring but is not the rate controlling.

The Boyd's film diffusion gives a linear fit that passes through the origin which indicates that intraparticle diffusion is the rate controlling mode of adsorption generally meaning that Pb^{2+} have to pass through the have to pass through the boundary layer and enters the internal pore network of the Ch-RBB.

These findings seem to be contradicting since IPD model revealed that it's not the rate determinant after its plot intersecting on the vertical axis, rather it significantly describes the nature of a good adsorbent being a multi-stage diffusion-controlled process i.e. both film and intraparticle diffusion control the process of adsorption at different stages (B. Liu et al., 2022). In the earlier stage, the IPD model captures film diffusion as the rate controlling process because Pb^{2+} must first interacts with the hydrodynamic external layer of the adsorbent making this film diffusion fast due to easily accessible adsorbent surface and good mixing speed. Later after some minutes, Pb^{2+} must go through the chitosan-coated mesopore layer to reach the internal NH_2 and COO- binding sites which is a slower process and hence dominant rate determinant step captured by Boyd model.

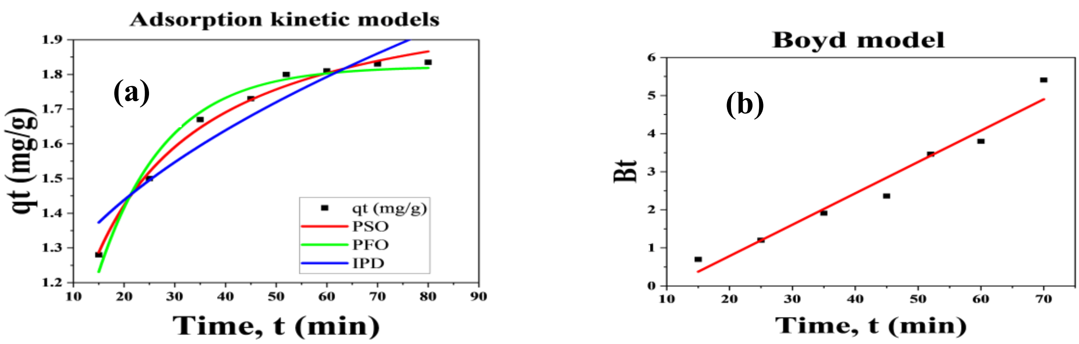

Figure 4.9: Kinetic models, (a) Non linear pseudo first, second and intraparticle diffusion, (b) Boyd model

5 CHAPTER 5

5.1 CONCLUSIONS

This study successfully synthesised and evaluated a chitosan modified rotten bagasse biochar as an effective adsorbent for the removal of Lead (II) ions from real industrial paint wastewater. SEM and FTIR characterisation results showed a high composition of mineral elements for the rotten bagasse biochar and increase in number of surface functional groups after chitosan modification suggestion ion exchanging and complexation respectively during adsorption. RSM-BBD model was statistically significant (F=32.21, p = 0.0007, R^2 = 0.9573). Optimal adsorption was obtained as 1.65g for adsorbent dosage, pH of 6.7, contact time of 80 minutes, predicted removal efficiency of 87.4% and an equilibrium adsorption capacity of 1.835 mg/g. Ch-RBBR demonstrated superior adsorption capacity relative to both pristine RBB of 1.23 mg/g and Ch-FBB of 1.49 mg/g, validating the dual benefit of natural pre-decomposition and biopolymer surface modification. The PSO model provided the best fit (R^2= 0.988) which confirmed chemisorption as the dominant rate-controlling mechanism and Boyd's model analysis indicated that film diffusion contributes to the controlling process in the initial stages of adsorption while pore diffusion at the later stage.

5.2 RECOMMENDATIONS

- The adsorption isotherm behaviour of Ch-RBB should be investigated by fitting Langmuir and Freundlich models to determine the maximum theoretical adsorption capacity and the nature of the adsorption surface whether homogeneous or heterogenous
- Thermodynamic parameters like enthalpies should be determined across a range of temperatures to establish whether the adsorption process is spontaneous, endothermic or exothermic in nature.
- Pilot-scale column adsorption experiments using fixed-bed reactors should be conducted to evaluate the breakthrough behaviour and dynamic adsorption capacity of Ch-RBB under continuous flow conditions.
- The pre-treatment of bagasse by aerobic decomposition to eliminate the production of methane (greenhouse gas).

REFERENCES

Adams, V. D. (2017). *Water and wastewater examination manual*. Routledge.

Akl, M. A., & Serage, A. A. (2024). Chitosan impregnated sugarcane bagasse biochar for removal of anionic dyes from wastewater. *Scientific Reports*, *14*(1), 27097. https://doi.org/10.1038/s41598-024-77708-9

Alharbi, T. (2023). Mapping of Groundwater, Flood, and Drought Potential Zones in Neom, Saudi Arabia, Using GIS and Remote Sensing Techniques. In *Water* (Vol. 15, Issue 5). https://doi.org/10.3390/w15050966

Ali, S., Naseer, S., Rehman, M., & Wei, Z. (2024). Recent trends and sources of lead toxicity: a review of state-of-the-art nano-remediation strategies. *Journal of Nanoparticle Research*, *26*(7), 168. https://doi.org/10.1007/s11051-024-06081-5

Alokika, Anu, Kumar, A., Kumar, V., & Singh, B. (2021). Cellulosic and hemicellulosic fractions of sugarcane bagasse: Potential, challenges and future perspective. *International Journal of Biological Macromolecules*, *169*, 564–582. https://doi.org/https://doi.org/10.1016/j.ijbiomac.2020.12.175

Amin, F. R., Huang, Y., He, Y., Zhang, R., Liu, G., & Chen, C. (2016). Biochar applications and modern techniques for characterization. *Clean Technologies and Environmental Policy*, *18*(5), 1457–1473.

Aniyikaiye, T. E., Oluseyi, T., Odiyo, J. O., & Edokpayi, J. N. (2019). Physico-Chemical Analysis of Wastewater Discharge from Selected Paint Industries in Lagos, Nigeria. In *International Journal of Environmental Research and Public Health* (Vol. 16, Issue 7, p. 1235). https://doi.org/10.3390/ijerph16071235

Bai, X., Zhang, M., Bingxuan, N., Zhang, W., Wang, X., Wang, J., Wu, D., Wang, L., & Jiang, K. (2022). *Journal of the Taiwan Institute of Chemical Engineers*, *132*, 104231. https://doi.org/10.1016/j.jtice.2022.104231

Bąk, J., Thomas, P., & Kołodyńska, D. (2022). Chitosan-Modified Biochars to Advance Research on Heavy Metal Ion Removal: Roles, Mechanism and Perspectives. In *Materials* (Vol. 15, Issue 17). https://doi.org/10.3390/ma15176108

Benalia, A., Atime, L., Baatache, O., Khalfaoui, A., Ghomrani, A. F., Derbal, K., Pizzi, A., Panico, A., Bouchareb, E. M., & Bouchareb, R. (2024). Removal of lead in water by coagulation flocculation process using Cactus-based natural coagulant: optimization and modeling by response surface methodology (RSM). *Environmental Monitoring and Assessment*, *196*(3), 244.

Benalia, M. C., Youcef, L., Bouaziz, M. G., Achour, S., & Menasra, H. (2022).. *Arabian Journal for Science and Engineering*, *47*(5), 5587–5599.

Bombuwala Dewage, N., Fowler, R. E., Pittman, C. U. J., Mohan, D., & Mlsna, T. (2018).

Lead (Pb(2+)) sorptive removal using chitosan-modified biochar: batch and fixed-bed studies. *RSC Advances*, *8*(45), 25368–25377. https://doi.org/10.1039/c8ra04600j

Burk, G. A., Herath, A., Crisler, G. B., Bridges, D., Patel, S., Pittman, C. U., & Mlsna, T. (2020). Cadmium and Copper Removal From Aqueous Solutions Using Chitosan-Coated Gasifier Biochar. *Frontiers in Environmental Science*, *Volume 8*-.

Charkiewicz, A. E., & Backstrand, J. R. (2020). file:///D:/DOWNLOADS/10.1007_s11270-019-4221-y-citation.ris. In *International Journal of Environmental Research and Public Health* (Vol. 17, Issue 12, p. 4385). https://doi.org/10.3390/ijerph17124385

Choudhary, M., Chakinala, N., Saini, P., Surolia, P. K., & Chakinala, A. G. (2025). Carbon foams derived from biomass with ultra-high adsorption capacity for the removal of tetracycline. *Materials Advances*.

Chowdhury, I. R., Chowdhury, S., Mazumder, M. A. J., & Al-Ahmed, A. (2022). Removal of lead ions (Pb2+) from water and wastewater: a review on the low-cost adsorbents. *Applied Water Science*, *12*(8), 185.

Collin, M. S., Venkatraman, S. K., Vijayakumar, N., Kanimozhi, V., Arbaaz, S. M., Stacey, R. G. S., Anusha, J., Choudhary, R., Lvov, V., Tovar, G. I., Senatov, F., Koppala, S., & Swamiappan, S. (2022). Bioaccumulation of lead (Pb) and its effects on human: A review. *Journal of Hazardous Materials Advances*, *7*, 100094. https://doi.org/https://doi.org/10.1016/j.hazadv.2022.100094

Debnath, B., Singh, W. S., & Manna, K. (2019). Sources and Toxicological Effects of Lead on Human Health. *Indian Journal of Medical Specialities*, *10*(2). https://journals.lww.com/imsp/fulltext/2019/10020/sources_and_toxicological_effects_of_lead_on_human.3.aspx

Divband Hafshejani, L., Hooshmand, A., Naseri, A. A., Mohammadi, A. S., Abbasi, F., & Bhatnagar, A. (2016). Removal of nitrate from aqueous solution by modified sugarcane bagasse biochar. *Ecological Engineering*, *95*, 101–111. https://doi.org/https://doi.org/10.1016/j.ecoleng.2016.06.035

El-Zahhar, A. A., Idris, A. M., Fawy, K. F., & Arshad, M. (2021). SEM, SEM-EDX, µ-ATR-FTIR and XRD for urban street dust characterisation. *International Journal of Environmental Analytical Chemistry*, *101*(7), 988–1006.

Emenike, E. C., Al-Senani, G. M., Al-Qahtani, S. D., Iwuozor, K. O., Egbemhenghe, A. U., & Adeniyi, A. G. (2026). Evaluating the effect of biomass condition on the properties of biochars derived from sweet lime fruit waste. *International Journal of Green Energy*, *23*(1), 232–244. https://doi.org/10.1080/15435075.2025.2546664

Ezeonuegbu, B. A., Machido, D. A., Whong, C. M. Z., Japhet, W. S., Alexiou, A., Elazab, S. T., Qusty, N., Yaro, C. A., & Batiha, G. E.-S. (2021). Lehmann, J., & Joseph, S. (Eds.). (2015). Biochar for Environmental Management: Science, Technology and Implementation (2nd ed.). Routledge. https://doi.org/10.4324/9780203762264. *Biotechnology Reports (Amsterdam, Netherlands)*, *30*, e00614.

https://doi.org/10.1016/j.btre.2021.e00614

Flávia Rezende Silva, A., Abner Rocha Lebron, Y., Almeida Ribeiro, L., Alice Dias Araujo, A., Coelho André, L., José Nunes de Paiva, M., Maciel D'auriol Souza, M., Koch, K., & Amaral, M. (2024). Thermophilic anaerobic membrane distillation bioreactor for sugarcane vinasse treatment- maximizing pollutants removal and resources recovery. *Chemical Engineering Journal*, *496*, 153680. https://doi.org/https://doi.org/10.1016/j.cej.2024.153680

Foo, K. Y., & Hameed, B. H. (2010). Insights into the modeling of adsorption isotherm systems. *Chemical Engineering Journal*, *156*(1), 2–10.

Gayathri, L. N., & Nair, P. (2023). Role of Aerobic and Anaerobic Bacteria in the Bio-conversion of Lignocellulose waste material. *Journal of Microbes and Research*, *2*(1), 2187–2836.

Goel, S. (2024). Physico Chemical and Biological Treatment Techniques for Lead Removal from Wastewater: A Review. *Lead Toxicity Mitigation: Sustainable Nexus Approaches*, 243–262.

He, Q., Hu, Z., Jiang, Y., Chang, X., Tu, Z., & Zhang, L. (2010). Preconcentration of Cu(II), Fe(III) and Pb(II) with 2-((2-aminoethylamino)methyl)phenol-functionalized activated carbon followed by ICP-OES determination. *Journal of Hazardous Materials*, *175*(1), 710–714. https://doi.org/https://doi.org/10.1016/j.jhazmat.2009.10.067

Hussain, M. N., Khudhair, A. F., & Ahmed, H. J. (2024). Evaluation of Lead Ion in the Wastewater of the Lifting and Treatment Stations Using ICP-MS and CPE Methods. *Indonesian Journal of Chemistry*, *24*(3), 715–728. https://doi.org/10.22146/ijc.87545

Inyang, M. I., Gao, B., Yao, Y., Xue, Y., Zimmerman, A., Mosa, A., Pullammanappallil, P., Ok, Y. S., & Cao, X. (2016). file:///D:/DOWNLOADS/S0165237022000675.ris. *Critical Reviews in Environmental Science and Technology*, *46*(4), 406–433. https://doi.org/10.1080/10643389.2015.1096880

Iroegbu, A. O. C., Teffo, M. L., Sadiku, E. R., Meijboom, R., & Hlangothi, S. P. (2025). Advancing wastewater treatment with green and scalable metal–organic frameworks: from synthetic strategies to real-world deployment. *Npj Clean Water*, *8*(1), 85. https://doi.org/10.1038/s41545-025-00514-x

Jasim, A. Q., & Ajjam, S. K. (2024). Removal of heavy metal ions from wastewater using ion exchange resin in a batch process with kinetic isotherm. *South African Journal of Chemical Engineering*, *49*(1), 43–54.

Joshi, M., Bhatt, D., & Srivastava, A. (2023). Enhanced adsorption efficiency through biochar modification: a comprehensive review. *Industrial & Engineering Chemistry Research*, *62*(35), 13748–13761.

Kumar, S., Chauhan, C., Sunidhi, Kumar, R., Kumar, J., & Aree, T. (2025). Immobilized

Mononuclear and Binuclear Copper (II) Complexes on Chitosan–PVA-Based Composite Films as Dip Catalyst for Dual Enzyme Mimicry. *ACS Applied Engineering Materials*.

Kumkum, P., & Kumar, S. (2024). A Review on Biochar as an Adsorbent for Pb(II) Removal from Water. *Biomass (Switzerland)*, *4*(2), 243–272. https://doi.org/10.3390/biomass4020012

Latha, S., Gomathi, T., Pavithra, S., Sudha, P. N., Nalluri, A., & Bhardwaj, P. (2023). Chitosan-based porous Carbon materials for agriculture and agro-waste applications. In *Handbook of Porous Carbon Materials* (pp. 763–812). Springer.

Li, Z., Huang, H., & Zhang, S. (2022). file:///D:/DOWNLOADS/S1631074812000318.risfile:///D:/DOWNLOADS/S1631074812000318.ris. *Journal of Analytical and Applied Pyrolysis*, *163*, 105497. https://doi.org/https://doi.org/10.1016/j.jaap.2022.105497

Liu, B., Finkel, M., & Grathwohl, P. (2022). First order approximation for coupled film and intraparticle pore diffusion to model sorption/desorption batch experiments. *Journal of Hazardous Materials*, *429*, 128314. https://doi.org/https://doi.org/10.1016/j.jhazmat.2022.128314

Liu, R., Zhang, Y., Hu, B., & Wang, H. (2022). Improved Pb(II) removal in aqueous solution by sulfide@biochar and polysaccharose-FeS@ biochar composites: Efficiencies and mechanisms. *Chemosphere*, *287*, 132087. https://doi.org/https://doi.org/10.1016/j.chemosphere.2021.132087

Liu, Y., Yan, J., Yuan, D., Li, Q., & Wu, X. (2013). file:///D:/DOWNLOADS/scholar (27).ris. *Chemical Engineering Journal*, *218*, 81–88.

Loc, N. X., Tuyen, P. T., Mai, L. C., & Phuong, D. T. (2022). Chitosan-Modified Biochar and Unmodified Biochar for Methyl Orange: Adsorption Characteristics and Mechanism Exploration. In *Toxics* (Vol. 10, Issue 9). https://doi.org/10.3390/toxics10090500

Luo, S., Li, X., Chen, L., Chen, J., Wan, Y., & Liu, C. (2014). Layer-by-layer strategy for adsorption capacity fattening of endophytic bacterial biomass for highly effective removal of heavy metals. *Chemical Engineering Journal*, *239*, 312–321. https://doi.org/https://doi.org/10.1016/j.cej.2013.11.029

Malool, M. E., Keshavarz Moraveji, M., & Shayegan, J. (2021). Optimized production, Pb(II) adsorption and characterization of alkali modified hydrochar from sugarcane bagasse. *Scientific Reports*, *11*(1), 22328. https://doi.org/10.1038/s41598-021-01825-y

Manyatshe, A., Cele, Z. E. D., Balogun, M. O., Nkambule, T. T. I., & Msagati, T. A. M. (2022). Chitosan modified sugarcane bagasse biochar for the adsorption of inorganic phosphate ions from aqueous solution. *Journal of Environmental Chemical Engineering*, *10*(5), 108243. https://doi.org/https://doi.org/10.1016/j.jece.2022.108243

Mastalerz, M., Drobniak, A., Briggs, D., & Bradburn, J. (2023). Variations in microscopic properties of biomass char: Implications for biochar characterization. *International Journal of Coal Geology*, *271*, 104235.

Mohanty, A. K., Vivekanandhan, S., Das, O., Romero Millán, L. M., Klinghoffer, N. B., Nzihou, A., & Misra, M. (2024). Biocarbon materials. *Nature Reviews Methods Primers*, *4*(1), 19.

Mukunda, C. K., Gurubasavaiah, K. M., & Banu, S. H. (2025). Early Release of Methane and Quicker Degradation of Bioplastics Using Activated Sludge. *Holistic Approach to Environment*, *15*(2), 57–68. https://doi.org/10.33765/thate.15.2.2

Nair K, S., Manu, B., & Azhoni, A. (2021). Sustainable treatment of paint industry wastewater: Current techniques and challenges. *Journal of Environmental Management*, *296*, 113105. https://doi.org/https://doi.org/10.1016/j.jenvman.2021.113105

Niu, G., Huang, Y., Hua, M., Wu, P., Li, J., Jia, C., Chao, Y., Liu, Z., & Zhu, W. (2024). Carboxyl carbon nanotubes strengthened tailorable chitosan imprinted polymers for selective adsorption of dibenzothiophene in hydrogenated diesel. *Chemical Engineering Journal*, *500*, 157044.

Nwajiaku, I. M., Olanrewaju, J. S., Sato, K., Tokunari, T., Kitano, S., & Masunaga, T. (2018). Change in nutrient composition of biochar from rice husk and sugarcane bagasse at varying pyrolytic temperatures. *International Journal of Recycling of Organic Waste in Agriculture*, *7*(4), 269–276.

Poonam, & Kumar, N. (2020). file:///D:/DOWNLOADS/S1385894713014848.risfile:///D:/DOWNLOADS/S1385894713014848.ris. *Environment, Development and Sustainability*, *22*(5), 4379–4406.

Raj, K., & Das, A. P. (2023). Lead pollution: Impact on environment and human health and approach for a sustainable solution. *Environmental Chemistry and Ecotoxicology*, *5*, 79–85. https://doi.org/https://doi.org/10.1016/j.enceco.2023.02.001

Ranjbar, Z., Pourhadadi, D., Montazeri, S., & Modaberi, M. R. (2023). Lead compounds in paint and coatings: a review of regulations and latest updates. *Progress in Organic Coatings*, *174*, 107247.

Revellame, E. D., Fortela, D. L., Sharp, W., Hernandez, R., & Zappi, M. E. (2020). Adsorption kinetic modeling using pseudo-first order and pseudo-second order rate laws: A review. *Cleaner Engineering and Technology*, *1*, 100032.

Salam, M. A., Al-Zhrani, G., & Kosa, S. A. (2012). Simultaneous removal of copper(II), lead(II), zinc(II) and cadmium(II) from aqueous solutions by multi-walled carbon nanotubes. *Comptes Rendus Chimie*, *15*(5), 398–408. https://doi.org/https://doi.org/10.1016/j.crci.2012.01.013

Sanjay, K., Anupam Kumar, G., & Professor, A. (2021). Lead Removal From Industrial Wastwater: a Review of Removal Mthods. *International Journal of Creative Research*

Thoughts, *9*(7), 2320–2882. www.ijcrt.org

Sharma, P., Sharma, S., Sharma, S. K., Jain, A., & Shrivastava, K. (2024). Review on recent advancement of adsorption potential of sugarcane bagasse biochar in wastewater treatment. *Chemical Engineering Research and Design*, *206*, 428–439.

Singh, A., Singh, S., Parashar, D., Kulshreshtha, N. M., Gaur, S., & Gupta, A. B. (2025). A Review on Sustainable Enhancement in Microbial Dynamics and Pollutant Removal in Constructed Wetlands: The Role of Agricultural Waste-Derived Biochar. *Water, Air, & Soil Pollution*, *236*(14), 897.

Singh, V., Singh, J., Singh, N., Verma, M. K., Praveena, S. M., & Mishra, V. (2024). Sustainable removal of Pb (II) from aqueous medium by using chitosan functionalized Citrus limetta peels biomass. *Bioremediation Journal*, *28*(3), 245–265.

Stark, J. S., Smith, J., King, C. K., Lindsay, M., Stark, S., Palmer, A. S., Snape, I., Bridgen, P., & Riddle, M. (2015). Physical, chemical, biological and ecotoxicological properties of wastewater discharged from Davis Station, Antarctica. *Cold Regions Science and Technology*, *113*, 52–62. https://doi.org/https://doi.org/10.1016/j.coldregions.2015.02.006

Su, C., Li, Z., Wang, W., Cheng, Z., Zheng, Z., & Chen, Z. (2022). Key Factors Dominating the Groundwater Chemical Composition in a Grain Production Base: A Case Study of Muling–Xingkai Plain, Northeast China. In *Water* (Vol. 14, Issue 14). https://doi.org/10.3390/w14142222

Sun, Y., Shi, X., Yang, Y., Suo, G., Zhang, L., Lu, S., & Chen, Z. (2022). Biomass-derived carbon for high-performance batteries: from structure to properties. *Advanced Functional Materials*, *32*(24), 2201584.

Thompson, C. O., Ndukwe, A. O., & Asadu, C. O. (2020). Application of activated biomass waste as an adsorbent for the removal of lead (II) ion from wastewater. *Emerging Contaminants*, *6*, 259–267.

Tigalana, D., Alunda, B. O., Ondiaka, M. N., Nibikora, I., Bongomin, O., & Lwanyaga, J. D. (2025). Lead (II) adsorption by KOH-modified rice straw biochar from battery wastewater: Adsorption optimization, isotherm, kinetic and thermodynamic studies. *Environmental Challenges*, 101371. https://doi.org/https://doi.org/10.1016/j.envc.2025.101371

Uchimiya, M., Lima, I. M., Thomas Klasson, K., Chang, S., Wartelle, L. H., & Rodgers, J. E. (2010). Immobilization of Heavy Metal Ions (CuII, CdII, NiII, and PbII) by Broiler Litter-Derived Biochars in Water and Soil. *Journal of Agricultural and Food Chemistry*, *58*(9), 5538–5544. https://doi.org/10.1021/jf9044217

Valenga, M. G. P., Gevaerd, A., Marcolino-Junior, L. H., & Bergamini, M. F. (2024). Biochar from sugarcane bagasse: Synthesis, characterization, and application in an electrochemical sensor for copper (II) determination. *Biomass and Bioenergy*, *184*, 107206.

Venzke, C. D., Rodrigues, M. A. S., Giacobbo, A., Bacher, L. E., Lemmertz, I. S., Viegas, C., Striving, J., & Pozzebon, S. (2017). Application of reverse osmosis to petrochemical industry wastewater treatment aimed at water reuse. *Management of Environmental Quality: An International Journal*, *28*(1), 70–77.

Verma, Y., Verma, A., Bhaskaralingam, A., Dhiman, P., Wang, T., Kumar, A., & Sharma, G. (2025). Application of Zero-Valent Iron and Its Derivatives in the Removal of Toxic Metal Ions from Groundwater. *Water*, *17*(10), 1524.

Vo, K. A., Xu, X. J., Li, T. G., Peng, R. H., Liu, S. L., & Yue, X. L. (2016). file:///D:/DOWNLOADS/scholar (23).ris. *Desalination and Water Treatment*, *57*(33), 15343–15352.

Wanyonyi, F. S., Orata, F., Mutua, G. K., Odey, M. O., Zamisa, S., Ogbodo, S. E., Maingi, F., & Pembere, A. (2024). Application of South African heulandite (HEU) zeolite for the adsorption and removal of Pb2+ and Cd2+ ions from aqueous water solution: Experimental and computational study. *Heliyon*, *10*(14).

Wojnárovits, L., Homlok, R., Kovács, K., Tegze, A., & Takács, E. (2024). Wastewater Characterization: Chemical Oxygen Demand or Total Organic Carbon Content Measurement? In *Molecules* (Vol. 29, Issue 2, p. 405). https://doi.org/10.3390/molecules29020405

Woldeamanuale, T. B., & Hassen, A. S. (2017). Toxicity study of heavy metals pollutants and physico-chemical characterization of effluents collected from different paint industries in Addis Ababa, Ethiopia. *J. Forensic Sci. Crim. Investig*, *5*, 555685.

Xie, Y., Zhou, G., Huang, X., Cao, X., Ye, A., Deng, Y., Zhang, J., Lin, C., & Zhang, R. (2022). Study on the physicochemical properties changes of field aging biochar and its effects on the immobilization mechanism for Cd2+ and Pb2+. *Ecotoxicology and Environmental Safety*, *230*, 113107.

Yahya, R., & Elshaarawy, R. F. M. (2024). Adsorptive removal of Pb (II) ions from aqueous effluents using O-carboxymethyl chitosan Schiff base-sugarcane bagasse microbeads. *International Journal of Biological Macromolecules*, *277*, 134350.

Yi, B., Guo, F., Wei, Q., Huang, F., Senadheera, S. S., Mašek, O., Sarmah, A. K., Rinklebe, J., & Ok, Y. S. (2025). Functionalized Biochar: Mechanisms of Oxygen-Containing Functional Groups in Water Pollutant Remediation. *ACS ES&T Water*, *5*(10), 5764–5784. https://doi.org/10.1021/acsestwater.5c00416

Yirdaw, G. (2025). Efficient removal of lead (II) from paint factory wastewater using Noug stalk activated carbon: A sustainable adsorption approach. *Heliyon*, *11*(3), e42281. https://doi.org/10.1016/j.heliyon.2025.e42281

Zhang, C., Li, M., & Wang, X. (2025). Characterization of magnetic chitosan-modified biochar and its adsorption of Zn2+ in electroplating rinsing wastewater. *Journal of Environmental Chemical Engineering*, *13*(3), 116501.

Zhang, R., Wilson, V. L., Hou, A., & Meng, G. (2015). Source of lead pollution, its influence on public health and the countermeasures. *International Journal of Health, Animal Science and Food Safety*, *2*(1).

Zhao, Q., Wang, Y., Xu, Z., & Yu, Z. (2021). Removal mechanisms of Cd (II) and Pb (II) from aqueous solutions using straw biochar: batch study, Raman and X-ray photoelectron spectroscopy techniques. *Desalination and Water Treatment*, *220*, 199–210.

Zhou, Y., Gao, B., Zimmerman, A. R., Fang, J., Sun, Y., & Cao, X. (2013). Sorption of heavy metals on chitosan-modified biochars and its biological effects. *Chemical Engineering Journal*, *231*, 512–518. https://doi.org/https://doi.org/10.1016/j.cej.2013.07.036

Zwolak, A., Sarzyńska, M., Szpyrka, E., & Stawarczyk, K. (2019). Sources of Soil Pollution by Heavy Metals and Their Accumulation in Vegetables: a Review. *Water, Air, & Soil Pollution*, *230*(7), 164. https://doi.org/10.1007/s11270-019-4221-y

APPENDICES

Appendix A: Biochar production process

Figure A.0.1: Biochar production process

Appendix B: Equipment used

(1)


(2)


Figure B.0.2&2: HI9146 Dissolved Oxygen meter and JEN WAY 6705 Vis Spectrophotometer

(3)


(4)


Figure B.3&0.3: Ex Stick EC500 Ph . Conductivity meter and Orbital Shaker SSL

Appendix C: Experiments

(5)  (6) 

FigureC.0.4&6: Extracting a yellow complex of $Pb(I)_2$ and Operating UV Vis's Spectrophotometer

(7)  (8) 

Figure C.7&8: Preparing Batch experiments and Assembling samples on orbital shaker

(9) 

FigureC.0.5: Filtration after adsorption experiments